Deep-Sea Research II 71-76 (2012) 32–48

Contents lists available at SciVerse ScienceDirect

Deep-Sea Research II

journal homepage: www.elsevier.com/locate/dsr2

Iron from melting glaciers fuels phytoplankton blooms in the Amundsen Sea (Southern Ocean): Phytoplankton characteristics and productivity

Anne-Carlijn Alderkamp [a,b,*], Matthew M. Mills [a], Gert L. van Dijken [a], Patrick Laan [c], Charles-Edouard Thuróczy [c], Loes J.A. Gerringa [c], Hein J.W. de Baar [b,c], Christopher D. Payne [d], Ronald J.W. Visser [b], Anita G.J. Buma [b], Kevin R. Arrigo [a]

[a] Department of Environmental Earth System Science, Stanford University, Stanford, CA 94305, USA
[b] Department of Ocean Ecosystems, University of Groningen, Nijenborg 7, 9747 AG, Groningen, The Netherlands
[c] Royal Netherlands Institute for Sea Research, P.O. Box 59, 1790 AB, Den Burg, Texel, The Netherlands
[d] Department of Earth and Ocean Sciences, University of British Columbia, Vancouver BC, Canada

ARTICLE INFO

Available online 16 March 2012

Keywords:
Phytoplankton
Photosynthesis
Primary productivity
Phaeocystis
Diatoms
Iron
Amundsen Sea
Pine Island Bay
Pine Island Glacier

ABSTRACT

The phytoplankton community composition and productivity in waters of the Amundsen Sea and surrounding sea ice zone were characterized with respect to iron (Fe) input from melting glaciers. High Fe input from glaciers such as the Pine Island Glacier, and the Dotson and Crosson ice shelves resulted in dense phytoplankton blooms in surface waters of Pine Island Bay, Pine Island Polynya, and Amundsen Polynya. Phytoplankton biomass distribution was the opposite of the distribution of dissolved Fe (DFe), confirming the uptake of glacial DFe in surface waters by phytoplankton. Phytoplankton biomass in the polynyas ranged from 0.6 to 14 μg Chl a L^{-1}, with lower biomass at glacier sites where strong upwelling of Modified Circumpolar Deep Water from beneath glacier tongues was observed. Phytoplankton blooms in the polynyas were dominated by the haptophyte *Phaeocystis antarctica*, whereas the phytoplankton community in the sea ice zone was a mix of *P. antarctica* and diatoms, resembling the species distribution in the Ross Sea. Water column productivity based on photosynthesis versus irradiance characteristics averaged 3.00 g C m^{-2} d^{-1} in polynya sites, which was approximately twice as high as in the sea ice zone. The highest water column productivity was observed in the Pine Island Polynya, where both thermally and salinity stratified waters resulted in a shallow surface mixed layer with high phytoplankton biomass. In contrast, new production based on NO_3 uptake was similar between different polynya sites, where a deeper UML in the weakly, thermally stratified Pine Island Bay resulted in deeper NO_3 removal, thereby offsetting the lower productivity at the surface. These are the first in situ observations that confirm satellite observations of high phytoplankton biomass and productivity in the Amundsen Sea. Moreover, the high phytoplankton productivity as a result of glacial input of DFe is the first evidence that melting glaciers have the potential to increase phytoplankton productivity and thereby CO_2 uptake, resulting in a small negative feedback to anthropogenic CO_2 emissions.

1. Introduction

Coastal polynyas are local areas of reduced ice cover that generally form due to offshore katabatic winds and seasonal ice melt. The reduced ice cover results in elevated irradiance in the water column in early spring. When the in situ irradiance increase coincides with a stable water column, it provides a light climate that is favorable for phytoplankton photosynthesis and growth, making Antarctic polynyas some of the most biologically productive regions of the Southern Ocean (Arrigo et al., 1999; Arrigo and van Dijken, 2003; Arrigo et al., 2008a, b). Phytoplankton primary productivity in polynyas is important for the support of biota who occupy higher trophic levels such as krill, penguins, and whales (Arrigo et al., 2003; Ainley et al., 2006). Moreover, polynyas play a disproportionally important role in sequestering anthropogenic CO_2 because of their high rates of primary production, rapid organic matter sinking fluxes (DiTullio et al., 2000), and formation of dense bottom waters (Arrigo et al., 2008a).

Phytoplankton productivity in Antarctic polynyas is generally dominated by diatoms and the haptophyte *Phaeocystis antarctica*

Abbreviations: AP, Amundsen Polynya; CDW, Circumpolar Deep Water; Chl *a*, Chlorophyll *a*; DFe, dissolved iron; E_{UML}, mean light level in the upper mixed layer; F_v/F_m, maximum efficiency of photosystem II; MCDW, Modified Circumpolar Deep Water; PAR, photosynthetically active radiation; *P–E*, photosynthesis versus irradiance; PIB, Pine Island Bay; PIG, Pine Island Glacier; PIP, Pine Island Polynya; POC, particulate organic carbon; PON, particulate organic nitrogen; z_{UML}, depth of the upper mixed layer; z_c, critical depth

* Corresponding author at: Department of Environmental Earth System Science, Stanford University, Stanford, CA 94305, USA.
E-mail address: Alderkamp@stanford.edu (A.-C. Alderkamp).

0967-0645/$ - see front matter © 2012 Elsevier Ltd. All rights reserved.
http://dx.doi.org/10.1016/j.dsr2.2012.03.005

(Prymnesiophyceae), although Cryptophytes, Chlorophyceae, and Prasinophyceae may also be abundant at certain times and regions (Arrigo et al., 1999; Wright et al., 2010; Kozlowski et al., 2011). The biogeochemical characteristics of these blooms differ in important ways (Arrigo et al., 1999). Previous data suggest that *P. antarctica* draws down twice as much CO_2 per mole of PO_4 removed than do diatoms (Arrigo et al., 1999). Other evidence suggests that *P. antarctica* is not readily grazed by microzooplankton (Caron et al., 2000; Tagliabue and Arrigo, 2003; Nejstgaard et al., 2007). Therefore, *P. antarctica* is thought to form the base of a marine food web that is substantially different from that supported by diatoms.

Phytoplankton primary productivity in the Southern Ocean is often limited by the availability of iron (Fe) (Boyd et al., 2007 and references therein), although light limitation due to deep vertical mixing below the critical depth may also limit phytoplankton growth (Mitchell et al., 1991; De Baar et al., 2005). The Fe supply for phytoplankton growth in polynyas is enhanced when compared to the open ocean due to input from melting sea ice (Sedwick and DiTullio, 1997; Lannuzel et al., 2010), floating icebergs (Raiswell et al., 2008; Raiswell, 2011; Shaw et al., 2011), upwelling Circumpolar Deep Water (CDW) (Klunder et al., 2011), and melting glaciers (Raiswell et al., 2006). Despite these enhanced sources, phytoplankton growth is often still seasonally Fe-limited following blooms in polynyas such as the Ross Sea (Sedwick and DiTullio, 1997; Sedwick et al., 2000; Arrigo et al., 2003; Tagliabue and Arrigo, 2005) and the Weddell Sea (Buma et al., 1991).

Satellite data revealed that the polynyas with highest productivity per surface area of Antarctica are found in the Amundsen Sea (Arrigo and van Dijken, 2003). The Amundsen Sea contains two polynyas, the Pine Island Polynya with a mean area of 17,632 km^2 in the east and Amundsen Polynya with a mean area of 27,333 km^2 in the west. The Amundsen Sea is located in the western Antarctic, where rates of ice sheet thinning are the highest in all of Antarctica (Pritchard et al., 2009) and are a potential Fe source for phytoplankton blooms (Raiswell et al., 2006, 2008). Several fast-flowing glaciers that are thinning rapidly drain into the Amundsen Sea, most notably the Pine Island Glacier (PIG), the Smith Glacier, and the Thwaites Glacier (Pritchard et al., 2009). The thinning of the ice sheets is mainly attributed to the regional bathymetry and oceanography. As the Antarctic Circumpolar Current (ACC) flows close to the continent, Circumpolar Deep Water (CDW) intrudes southward through deep troughs onto the Antarctic continental shelf as modified CDW (MCDW) (Jacobs et al., 1996, 2011; Jenkins et al., 1997; Hellmer et al., 1998; Walker et al., 2007; Nitsche et al., 2007). This relatively warm (~1.2 °C) and salty MCDW is able to enter the cavity beneath the floating terminus of the PIG and drive basal melting (Jenkins et al., 2010; Jacobs et al., 2011). The resulting seawater dilution by the glacial melt initiates a circulation pattern whereby fresher and cooler meltwater MCDW flows up the underside of the floating ice sheets and returns to the open sea higher in the water column (Hellmer et al., 1998).

During the 2009 DynaLiFe program, an international collaboration that was part of the International Polar Year, we found that meltwater MCDW from the PIG and other glaciers draining into the Amundsen Sea polynyas is the major source of Fe for the phytoplankton blooms in these polynyas (Gerringa et al., 2012). Here, we describe the characteristics of the phytoplankton bloom that was fueled by this Fe input, including phytoplankton community composition, photo-physiological characteristics, and primary productivity of this highly productive area.

2. Methods

2.1. Sampling

Seawater samples were collected during the NBP 09-01 cruise on the RVIB *Nathaniel B. Palmer* in the Amundsen Sea area during the austral summer, 12 January–17 February 2009 (Figs. 1 and 2). We entered a band of multi- and first-year ice to the north of Pine Island Polynya (PIP) on 12 January and followed a depression in the continental shelf through the sea ice (Sta 2, 3, 5, 7, 10) into the PIP. We transected the PIP on 15 and 16 January (Sta 11, 12, 13, 14) and subsequently sampled the PIB (Sta 36, 37, 46, 47, 86, 88, 89, 90, 94, 99) and stations in proximity to the PIG tongue (Sta 16,

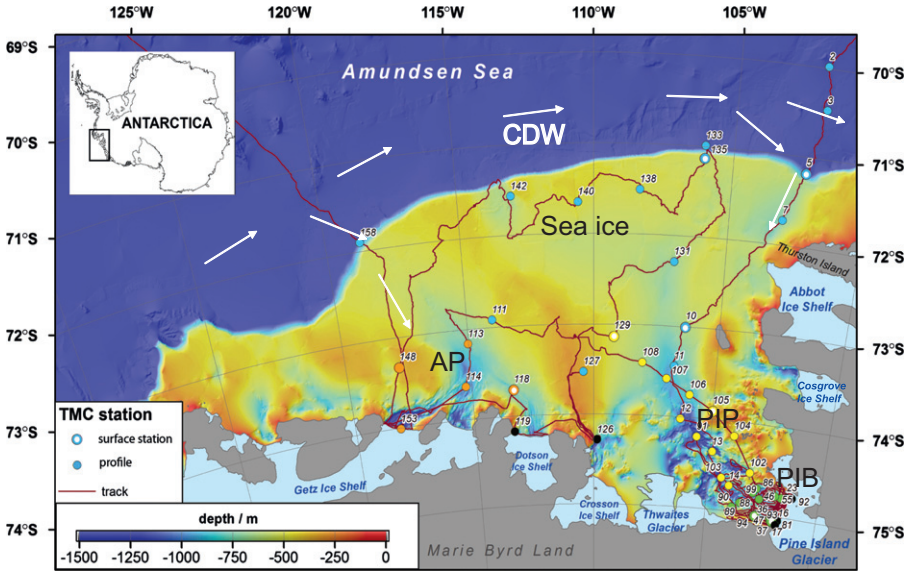

Fig. 1. DynaLiFe cruise track and stations superimposed on the bathymetry of the Amundsen Sea by Nitsche et al. (2007). White arrows indicate the flow of Circumpolar Deep Water (CDW) to the east in the Antarctic Circumpolar Current and south, where it flows onto the continental shelf through troughs in the shelf as modified CDW (MCDW). Blue stations were located in the sea ice zone, yellow stations in the Pine Island Polynya (PIP), green stations in the Pine Island Bay (PIB), orange stations in the Amundsen Polynya (AP), and black stations were influenced by outflow of meltwater MCDW from under glacier tongues. (For interpretation of the references to color in this figure legend, the reader is referred to the web version of this article.)

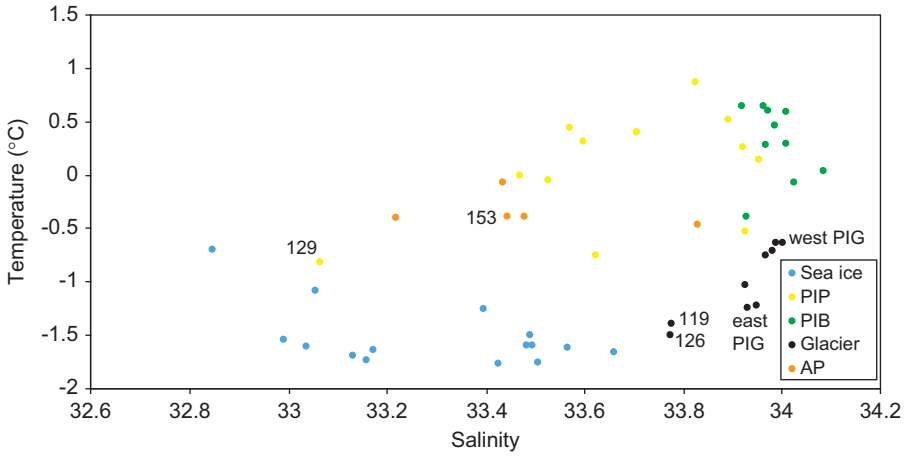

Fig. 2. Temperature versus salinity characteristics of surface waters (10 m) of the stations in different geographical regions of the sea ice, Pine Island Polynya (PIP), Pine Island Bay (PIB), Amundsen Polynya (AP), and glacier sites. Stations of interest are marked.

17, 81, 93 on the western end, 23, 55, 92 on the eastern end). On 31 January, we sampled another transect through the PIP (Sta 102, 104, 105, 106, 107, 108, and 129 on 6 February). From 1 to 14 February, we sampled the Amundsen Polynya (AP) (113, 114, 118, 148) and stations in proximity to the Dotson (Sta 119), Crosson (Sta 126), and Getz (Sta 153) ice shelves. From 8–15 February, we sampled stations in the sea ice zone (Sta 127, 131, 133, 135, 138, 140, 142, 158).

Continuous vertical profiles of temperature, salinity, irradiance, fluorescence, and suspended particle abundance were obtained from the water column using a SeaBird 911+CTD, a Chelsea fluorometer, photosynthetically active radiation (PAR) sensor (Biosperical), and a 25-cm WetLab transmissometer, respectively, on a cast preceding collection of water samples. Water was sampled during daylight hours from discrete depths in the upper 300 m of the water column with 12 L GoFLO bottles using trace metal clean (TMC) techniques (Gerringa et al., 2012). Sampling depths were typically 10, 25, 50, 100, 200, and 300 m. Temperature, salinity, and derived density data were binned at one meter intervals.

Samples were collected for dissolved Fe (DFe), total dissolvable Fe (TDFe) (Gerringa et al., 2012), nutrients, pigment composition, particulate organic carbon (POC), particulate organic nitrogen (PON), photosynthesis versus irradiance (*P–E*) relationships, phytoplankton absorption, and fluorescence analysis.

2.1.1. Nutrients

Samples for determination of phosphate (PO_4) and nitrate+nitrite (NO_3+NO_2) were filtered through Whatman GF/F filters and frozen until analysis on a WestCo SmartChem 200 discrete autoanalyzer. NO_3+NO_2 is presented as NO_3, as the contribution of NO_2 is negligible in Antarctic waters.

2.1.2. POC and PON

Duplicate samples for POC and PON were filtered onto precombusted (450 °C for 4 h) 25 mm Whatman GF/F filters and dried at 60 °C until analysis on a Carlo-Erba NA-1500 elemental analyzer using acetanilide as a calibration standard.

2.1.3. Photosynthesis vs. irradiance (P–E)

P–E relationships were determined using the ^{14}C-bicarbonate incorporation technique by incubation of 2 mL aliquots in a photosynthetron for one hour over a range of 20 different light intensities ranging from 3 to 542 µmol quanta $m^{-2}\,s^{-1}$ at 2 °C (Lewis and Smith, 1983; Arrigo et al., 2010). Carbon uptake normalized by chlorophyll *a* (Chl *a*) concentration was calculated from radioisotope incorporation and the data were fitted by least squares nonlinear regression to the equation of Webb et al. (1974) to which the P_o^* term was added representing CO_2 uptake or release in the dark (Arrigo et al., 2010):

$$P^* = P_m^*\left(1-\exp\left(-\alpha^*\frac{E}{P_m^*}\right)\right)-P_o^* \quad (1)$$

where P_m^* is the maximum rate of CO_2 fixation and α^* is the initial slope of the *P–E* curve (g C g^{-1} Chl *a* h^{-1} [µmol quanta $m^{-2}\,s^{-1}$]$^{-1}$). The photoacclimation parameter, E_k, was calculated as P_m^*/α^*. CO_2 incorporation was also fitted to the model of Platt et al. (1980), which contains the photoinhibition parameter ß* (g C g^{-1} Chl *a* hr^{-1} [µmol quanta $m^{-2}\,s^{-1}$]$^{-1}$). However, ß* was not significant in any of the *P–E* curves and, therefore, this model was disregarded. Due to methodological difficulties, *P–E* relationships were only determined at Sta. 104 and later.

2.1.4. Phytoplankton absorption

Aliquots of the seawater sample (15 mL) were filtered onto GF/Fs for the measurement of particulate absorption spectra (a_p, 300–800 nm) on a Perkin-Elmer Lambda 35 spectrophotometer equipped with an integrating sphere (Labsphere) using the filter pad method and optical corrections in Mitchell and Kiefer (1988) and the coefficients of Bricaud and Stramski (1990). Detrital absorption (a_{det}, 300–800 nm) was assayed after methanol extraction according to the method of Kishino et al. (1985). Chl *a*-specific phytoplankton absorption (a_{ph}^*) at each wavelength (λ) was calculated as

$$a_{ph}^*(\lambda) = \frac{a_p(\lambda)-a_{det}(\lambda)}{[Chla]} \quad (2)$$

where [*Chla*] is the Chl *a* concentration of the sample.

Spectrally weighted mean Chl *a*-specific absorption coefficients ($\overline{a}^*$, m^2 mg Chl a^{-1}) were calculated using the equation

$$\overline{a}^* = \frac{\sum_{400}^{700} a_{ph}^* E(\lambda)}{\sum_{400}^{700} E(\lambda)} \quad (3)$$

where $E(\lambda)$ (µmol quanta $m^{-2}\,s^{-1}$) is the spectral irradiance of the photosynthetron.

The quantum yield of photosynthesis (Φ_m) was calculated as

$$\Phi_m = \frac{\alpha^*}{43.2\overline{a}^*} \quad (4)$$

after first confirming that Φ_m was maximal at the lowest light level used in each of the assays (Johnson and Barber, 2003).

2.1.5. Pigment analysis

To determine the Chl *a* concentration of each sample, 10–500 ml of seawater was filtered onto 25 mm GF/F filters (Whatman), extracted overnight in 5 ml of 90% acetone, and analyzed on a Turner Model 10AU Fluorometer before and after acidification (Holm-Hansen et al., 1965).

For HPLC analysis of phytoplankton pigments, 50–1000 ml of seawater was filtered onto 25 mm GF/F filters, snap-frozen in liquid nitrogen, and stored at −80 °C until analysis within 6 months of collection. The filters for pigment analysis were then freeze-dried (48 h) and extracted in 90% acetone (48 h). Pigments were separated on a HPLC system (Waters 2690 separation module, 996 photodiode array detector) using a C_{18} 5 μm Delta-Pak reverse-phase column (Kraay et al., 1992; Van Leeuwe et al., 2006). Quantification was done using standard dilutions of Chl *a*, chlorophyll *b* (Chl b), chlorophyll c_3 (Chl c_3), 19′ butanoyloxyfucoxanthin (19′-But), fucoxanthin (Fuc), 19′ hexanoyloxyfucoxanthin (19′-Hex), diadinoxanthin (DD), diatoxanthin (DT), and ß-carotene (ß-Car). The Chl *a* breakdown/intermediate product, chlorophyllide *a*, was analyzed and detected in low concentrations (< 10% of Chl *a*) in seven stations only and are therefore not presented.

2.1.6. Fluorescence measurements

The maximum photochemical efficiency of photosystem II (F_v/F_m) was determined using a pulse amplified modulated (PAM) fluorometer (Water PAM, Heinz Walz, GmBH) at 2 °C. Prior to analysis, the PAM was blanked with GF/F-filtered seawater from the same station (Cullen and Davis, 2003). After sampling from the GoFLO bottles, samples were acclimated in the dark at 2 °C for 30 min to fully oxidize the photosynthetic reaction centers. The minimum fluorescence (F_o) and maximum fluorescence (F_m) were measured on triplicate 4 mL subsamples. F_o was determined using the measuring (non-photochemistry-inducing) light of the PAM and F_m was measured by applying a saturating light pulse of 4000 μmol quanta m^{-2} s^{-1} for 0.8 ms to close all PS II reaction centers. The maximum dark-acclimated efficiency of PSII (F_v/F_m) was calculated as (Krause and Weis, 1991):

$$F_v/F_m = \frac{F_m - F_o}{F_m}. \quad (5)$$

2.2. Data analysis

2.2.1. Diffuse attenuation coefficient

The attenuation of downwelling PAR in the water column (K_d) was determined by fitting the equation:

$$E_z = E_0 e^{-Kd*z} \quad (6)$$

to each PAR profile, where E_z is the irradiance at depth z and E_0 is the irradiance just below the sea surface.

2.2.2. Euphotic zone

K_d was used to calculate the depth of the euphotic zone, z_{EU}, defined as the depth at which the downwelling PAR falls to 1% of the value just below the sea surface (Kirk, 1994):

$$z_{EU} = \frac{\ln(0.01)}{K_d[PAR]}. \quad (7)$$

2.2.3. Critical depth

The critical depth (z_c) is the depth above which vertically integrated rates of phytoplankton photosynthesis and community respiration are equal. To determine z_c, a reformulation of the original (Sverdrup, 1953) equation suggested by Nelson and Smith (1991) for the Southern Ocean was used (see also Strutton et al., 2000):

$$z_c = \sum \frac{E_0}{3.78K_d}. \quad (8)$$

2.2.4. Upper mixed layer depth

We defined the depth of the upper mixed layer (z_{UML}) as the shallowest depth at which the density (σ_T) exceeded the surface density by 0.02 kg m^{-3} (Cisewski et al., 2008. The choice of 0.02 as value for $\Delta\ \sigma_T$ is somewhat arbitrary, as some studies have used greater values (Long et al., 2011). In this study choosing a greater value for $\Delta\ \sigma_T$ would only have affected the z_{UML} in some glacier stations close to ice shelves, meltwater MCDW and vigorous vertical mixing was observed (Gerringa et al., 2012).

2.2.5. Mean daily PAR in the upper mixed layer

To calculate the total daily PAR in the upper mixed layer (E_{UML}, mol quanta m^{-2} day^{-1}), we used the equation of (Riley, 1957):

$$E_{UML} = \frac{\overline{E}_{surf} T(1 - e^{-K_d z_{UML}})}{K_d z_{UML}} \quad (9)$$

where $\overline{E}_{surf}$ is the total daily surface PAR averaged over five days and T is the mean transmittance through the sea surface (0.85 for open water, 0.20 for gray ice and nilas, and 0.05 for snow covered and multiyear ice; Allison et al., 1993).

2.2.6. Phytoplankton community composition based on CHEMTAX analysis

The CHEMTAX analysis package, version 1.95 (Mackey et al., 1996; Wright et al., 1996) was used to assess phytoplankton class abundance. The initial database contained specific pigment signatures for six phytoplankton classes that generally dominate Antarctic waters (Wright et al., 2010), including Chlorophytes, Prasinophytes, Cryptophytes, diatoms (with a separate category for *Pseudonitzschia*), and two classes of *P. antarctica*. The pigment signature of *P. antarctica* is variable (Zapata et al., 2004) and changes in response to Fe-limitation (Van Leeuwe and Stefels, 2007; DiTullio et al., 2007; Alderkamp et al., 2012). Based on published ratios of Fuc, 19′-Hex, and 19′-Fuc, separate classes of nutrient-replete and Fe-limited *P. antarctica* were distinguished (Table 1; Wright et al., 2010; Alderkamp et al., 2012). After analysis, Prasinophytes and Chlorophytes were pooled as green algae and presented together with Cryptophytes because of their low abundance, whereas *Pseudonitzschia* and other diatoms were

Table 1
Pigment:Chl *a* ratios used in CHEMTAX analysis of pigment data: (a) initial ratios (modified from Wright et al. (2010)), (b) optimized ratios after analysis.

	Chl c_3	*19′-But*	*19′-Hex*	*Fuc*	*Alx*	*Chl b*
(a)						
Prasinophytes	0	0	0	0	0	0.620
Cryptophytes	0	0	0	0	0.220	0
Chlorophytes	0	0	0	0	0	0.180
Diatoms	0	0	0	0.520	0	0
Pseudonitzschia	0.033	0	0	0.610	0	0
P. antarctica + Fe	0.130	0.01	0.410	0.080	0	0
P. antarctica − Fe	0.270	0.001	1.100	0.010	0	0
(b)						
Prasinophytes	0	0	0	0	0	0.383
Cryptophytes	0	0	0	0	0.180	0
Chlorophytes	0	0	0	0	0	0.153
Diatoms	0	0	0	0.342	0	0
Pseudonitzschia	0.040	0	0	0.415	0	0
P. antarctica + Fe	0.171	0.017	0.294	0.057	0	0
P. antarctica − Fe	0.372	0.001	0.376	0.004	0	0

pooled and presented as diatoms because of their functional similarity.

2.2.7. New production

New production (NP) was estimated using the calculated NO_3 deficit ($\Delta[NO_3]$), similar to that used previously in the Ross Sea (Sweeney et al., 2000; Arrigo et al., 2000; Smith and Asper, 2000; Smith et al., 2006):

$$\Delta[NO_3] = \int_0^z [NO_3]_{MCDW} dz - \int_0^z [NO_3]_{sal} dz \quad (10)$$

where $[NO_3]_{sal}$ is the salinity-corrected NO_3 concentration at depth z and $[NO_3]_{MCDW}$ is the mean NO_3 concentration of 30.31 μM at a salinity of 34.16 of the meltwater MCDW upwelling water from under the PIG. To calculate cumulative new production since December 1, production calculated in N units was converted to C units using the mean molar C/N ratio of particulate matter measured in the study region. All integrations were from 0–100 m. Below this depth, winter water (WW) was observed in the PIP (Gerringa et al., 2012). The mean NO_3 concentrations in this WW layer were lower than the concentrations in the MCDW upwelling from under the PIG, and low levels of fluorescence were detected, indicating that phytoplankton may have taken up some NO_3. The potential remineralization of NO_3 via nitrification was ignored, since this process is extremely slow at the low temperatures of the Antarctic shelf waters (Karl et al., 1996). This estimation ignores lateral advection of water masses, which is discussed in Section 4.

2.2.8. Export production

Depth-integrated PON was compared to the depth-integrated NO_3 deficit, and the difference was considered to be an estimate of export production from the beginning of the bloom to the date of sampling. This method ignores the fraction of NO_3 that would have entered the dissolved organic nitrogen (DON) pool, which is small in Antarctic waters (Smith and Asper, 2000). Similar to the NP calculations, effects of lateral advection were ignored.

2.2.9. Water column phytoplankton productivity

This property was estimated from the Chl *a* concentrations and light availability in the water column using the measured *P–E* parameters. At depth intervals of 1 m, Chl *a* concentrations were estimated from continuous vertical fluorescence profiles that were calibrated to the measured Chl *a* concentrations at similar depths (Chl *a* [μg L^{-1}]=0.52∗fluorescence [arb units] (R^2=0.80). The daily light

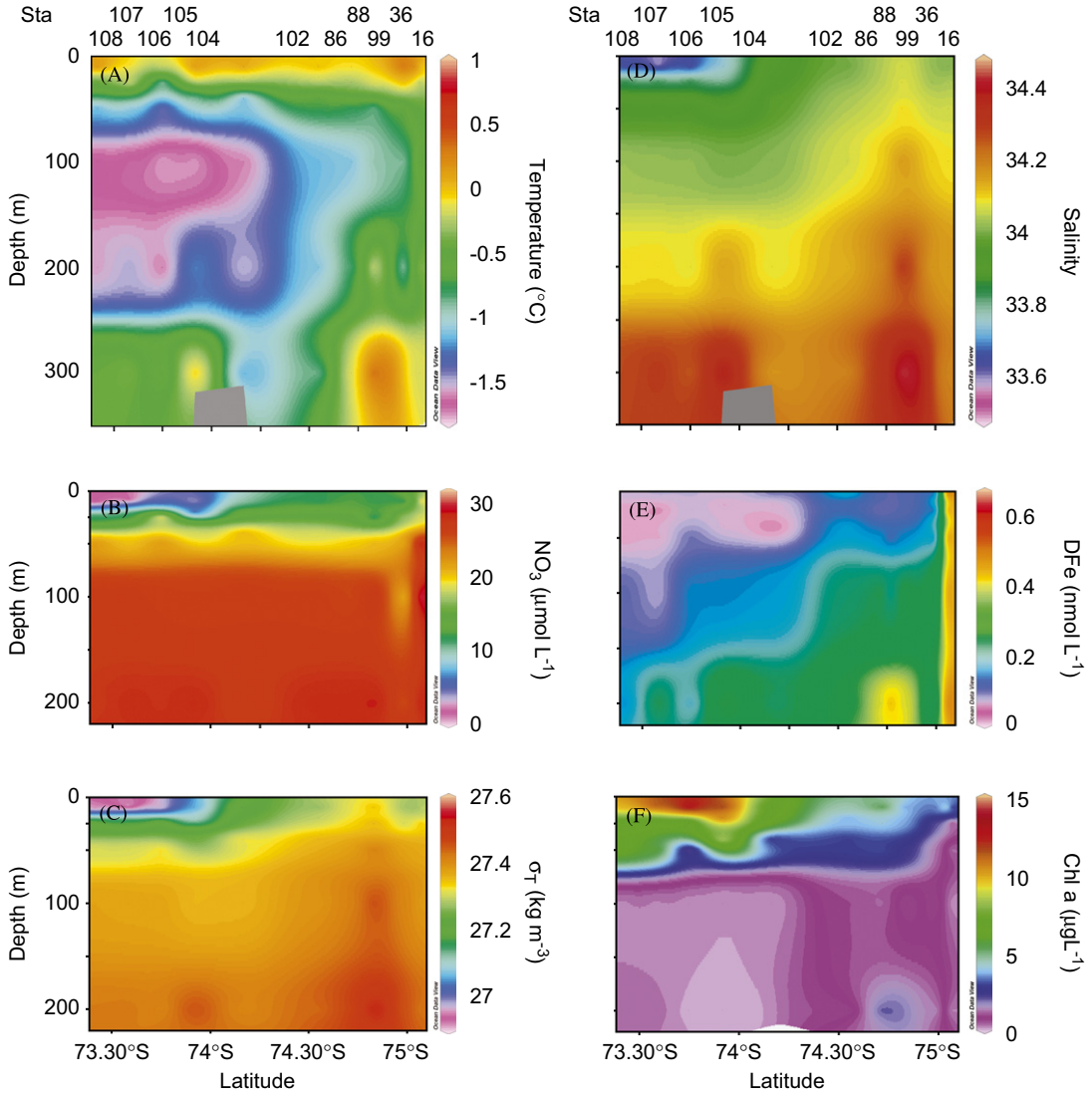

Fig. 3. Section plots of water properties of the stations on a transect from the southwestern end of the PIG (Sta 16) to the northwest, transecting the PIB and the PIP (Sta 104–108). (A) Temperature, (B) Nitrate+nitrite concentration, (C) Density (σ_T), (D) Salinity, (E) Dissolved iron (DFe) concentration, and (F) Chl *a* concentration.

cycle was binned in 10 min intervals and the mean over the previous five days was used to estimate the sinusoidal light cycle at 1 m depth intervals at each station based on the measured K_d of that station. These light levels were then used to calculate the phytoplankton productivity at each depth using *P–E* parameters of the phytoplankton at 10 m depth of the station. Since no *P–E* curves were available for the PIB, mean *P–E* parameters of the PIP and AP were used to estimate productivity there.

2.2.10. Statistical analysis

Data were checked to see if they were normally distributed. If they were, one-way ANOVA tests were used to compare the mean of hydrographic variables and biological parameters from different regions. If distributions were not normal, the non-parametric Mann-Whitney *U* test was used. Differences were considered significant at $p < 0.05$.

3. Results

3.1. General characteristics of the study region

The hydrography in the study area was driven by MCDW flowing onto the continental shelf, characterized by temperatures of 1.2 °C and salinities > 34.6, which was detected in the central PIP at depths below 300 m. Above this stratum, a winter water (WW) layer with a temperature of −1.79 to −1.68 °C and a salinity of 34.01 was observed between 50 and 200 m. At the western end of the tongue of the PIG, meltwater MCDW outflow and upwelling from under the glacier was observed throughout the upper 300 m of the water column (Fig. 3A and D, Gerringa et al., 2012). This meltwater MCDW in surface waters was fresher (salinity ~34.0) and colder (temperature < −0.5 °C) than the MCDW flowing onto the shelf, indicating basal melting of the glacier tongue. Upwelling/outflow of meltwater MCDW was also observed at the eastern end of the PIG (Sta. 23 and 92) and close to the Crosson (Sta. 126) and Dotson (Sta. 119) ice shelves (Fig. 2). However, meltwater MCDW was not detected close to the Getz Ice Shelf (Sta. 153), where the water was fresher (salinity ~34.4) and warmer (temperature −0.3 °C). Therefore, this station was classified as an Amundsen polynya (AP) station.

We encountered a dense phytoplankton bloom in surface waters of the PIP, PIB, and AP that had started around 10 December in both polynyas, as revealed by satellite ocean color data (Arrigo et al., 2012). The transect into the PIP on 15 January took place near the peak in Chl *a* and primary production (Arrigo et al., 2012), which lasted for approximately two weeks. The second transect through the PIP on 30 and 31 January took place just before Chl *a* began to decline. In the AP, Chl *a* peaked earlier than in the PIP (beginning of January) and the phytoplankton bloom was already in decline when we sampled the AP on 2, 3, 14, and 15 February.

3.2. Regional variability in phytoplankton characteristics

Here we describe the characteristics of the phytoplankton blooms in five different regions of the Amundsen Sea (Figs. 1 and 2), including (1) glacier sites less than 5 km from the PIG and the Crosson and Dotson ice shelves, (2) the PIB adjacent to the PIG, (3) the PIP, (4) the AP, and (5) the sea ice stations (stations with > 50% ice cover). In addition, a vertical section through the phytoplankton bloom extending from the western end of the PIG to the northwest into the PIB and PIP is used to characterize horizontal and vertical gradients in hydrography and phytoplankton characteristics from the PIG northward to the open ocean.

3.2.1. Glacier sites

The water column at each of the glacier sites near the PIG, Crosson, and Dotson ice shelves was characterized by little to no stratification in the upper 300 m. Outflowing meltwater MCDW at a mean salinity of 33.92 and mean temperature of −1.01 °C to −0.64 °C was observed in surface waters of these sites (Fig. 2, Table 2). At most stations, the z_{UML} was deep relative to other regions, exceeding 70 m (Table 2, Fig. 4C), and resulted in a relatively low E_{UML} in some stations. However, due to the low K_d at most glacier sites, the z_c was deeper than z_{UML} at all glacier stations and the mean E_{UML} of glacier sites was 8.0 mol quanta m^{-2} d^{-1}, similar to values in the PIB, AP, and ice stations (Table 2).

Phytoplankton biomass was very low throughout the water column at the glacier sites, with surface Chl *a* concentrations usually below 1 μg L^{-1} (Table 3, Fig. 4F). The concentrations of macronutrients were similar to those in the CDW, with mean NO_3 concentrations of 30.31 μmol L^{-1}. DFe was high throughout the water column (Gerringa et al., 2012), with mean surface concentrations of 0.62 nmol L^{-1}, exceeding those in our other study regions. The high nutrient and low Chl *a* concentrations indicate little accumulation of phytoplankton in these waters since the beginning of the season. At stations with a deep z_{UML}, low E_{UML} may have hampered phytoplankton growth, although z_{UML} was shallower than z_c in all stations, indicative of light conditions favorable for phytoplankton net growth. More likely, outflow and upwelling of meltwater MCDW flowing from beneath the glacier termini may have diluted surface waters with deeper water having high DFe and NO_3 concentrations and low phytoplankton biomass.

3.2.2. Pine Island Bay

The surface waters of the PIB were characterized by relatively high salinity compared to the PIP and AP (mean 33.99, Table 2, Fig. 3D), similar to that of surface waters of the glacier stations and indicative of MCDW with little modification by sea-ice melt. Waters in the upper 20 m of the PIB were warmer than both deeper waters (Fig. 3A) and surface waters at glacier sites (Fig. 2, Table 2), indicative of solar warming. Thermal stratification resulted in a relatively deep z_{UML} (mean 22.3 m, Table 2, Fig. 4C), which, in combination with an intermediate K_d, resulted in a value for E_{UML} that was similar to our other study regions (Table 2). The z_{UML} was shallower than the z_c in all PIB stations.

Surface phytoplankton biomass was relatively high and constant over the PIB (2.9–5.1 μg L^{-1} Chl *a*, Fig. 4F) and evenly

Table 2
Mean and standard deviation of properties of the water column and surface waters (10 m) of the glacier sites, Pine Island Bay, Pine Island Polynya, Amundsen Polynya, and sea ice stations. Means are significantly different at the $p < 0.05$ level unless connected by the same letter.

	n	z_{UML} (*m*)	K_d	z_{EU} (*m*)	z_c (*m*)	E_{UML} (mol quanta m^{-2} d^{-1})	$T_{surface}$ (°C)	$S_{surface}$	σ_T
Glacier	9	75.4^{c} (38.1)	0.113^{a} (0.04)	45.4 (14.5)	166.6 (73.4)	8.2^{b} (4.4)	−1.01 (0.34)	33.92^{a} (0.09)	27.28^{a} (0.06)
Pine Island Bay	10	22.3^{a} (5.8)	0.29^{bc} (0.09)	16.8 (4.2)	63.2^{a} (18.1)	10.0^{ab} (5.4)	0.31^{a} (0.35)	33.99^{a} (0.05)	27.27^{a} (0.05)
Pine Island Polynya	13	15.2^{b} (6.7)	0.36^{c} (0.10)	13.9 (4.3)	56.5^{a} (17.6)	13.1^{a} (5.2)	0.09^{ab} (0.5)	33.67^{b} (0.25)	27.03^{bc} (0.19)
Amundsen Polynya	5	36.2^{ac} (26.6)	0.24^{b} (0.07)	20.9 (7.5)	64.5^{a} (24.3)	7.6^{ab} (4.6)	-0.34^{b} (0.15)	33.48^{bc} (0.22)	26.89^{c} (0.18)
Sea ice	15	15.7^{b} (6.1)	0.18^{a} (0.09)	33.9 (18.5)	106.8 (54.6)	10.3^{ab} (4.5)	−1.51 (0.29)	33.29^{c} (0.25)	26.78^{b} (0.21)

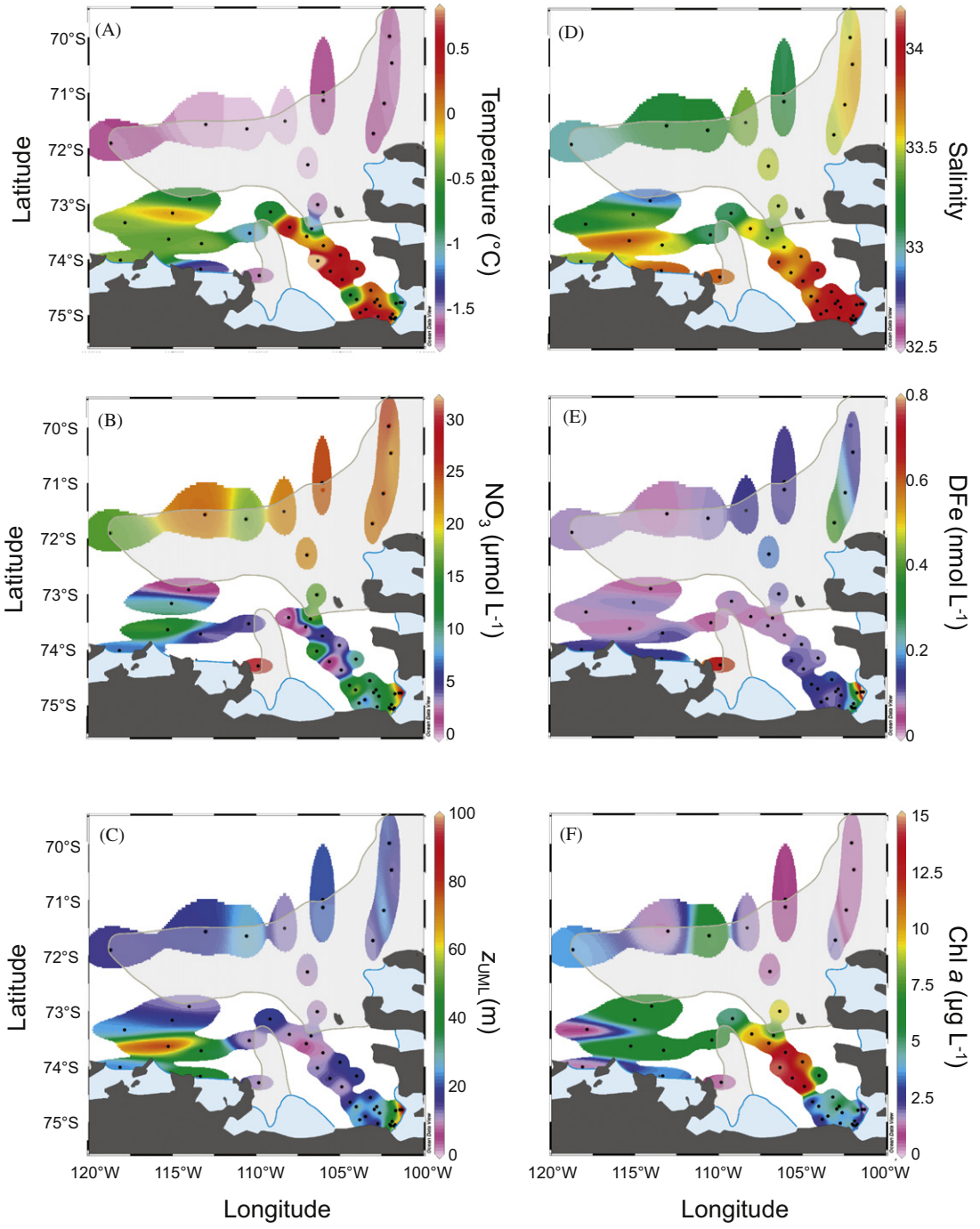

Fig. 4. Characteristics of surface water properties (10 m) of the Amundsen Sea with the >50% sea ice concentration at the time of sampling nearby stations shaded in gray. Ice shelves are light blue whereas land is gray. (A) Temperature, (B) Nitrate+nitrite concentration, (C) Depth of the upper mixed layer (z_{UML}), (D) Salinity, (E) Dissolved iron (DFe) concentration, and (F) Chl *a* concentration. (For interpretation of the references to color in this figure legend, the reader is referred to the web version of this article.)

distributed through the UML (Fig. 3F). The mean surface (10 m) concentrations of NO_3 and PO_4 were moderate throughout the PIB (9.96 µmol L^{-1} and 0.85 µmol L^{-1}, respectively, Table 3, Fig. 3B), as were concentrations of DFe (0.13 nmol L^{-1}, Table 3, Fig. 4B).

P. antarctica dominated the phytoplankton bloom in the PIB, comprising up to 92% of the phytoplankton community in surface waters (Table 4, Fig. 6A), as determined by CHEMTAX analysis on the pigment composition. The phytoplankton community composition in the PIB showed little or no vertical structure, with *P. antarctica* dominating the entire upper 100 m of the water column (Fig. 5A). The contribution of diatoms to the phytoplankton community was <10%, except at Sta. 94 located in the southwest of the PIB, where they contributed 19%. Concentrations of Chl *b* (indicative of Prasinophytes and Chlorophytes) and Alx (present in Cryptophytes) were below detection limits in the PIB. Based on the effects of low Fe concentrations on the *P. antarctica* pigment composition, we distinguished two separate *P. antarctica* groups, one with a low-Fe and one with a high-Fe pigment signature. On average, 52% of the surface *P. antarctica* population exhibited the high-Fe pigment signature (Table 4, Fig. 6D), which increased at greater depths (Fig. 5D). The mean F_v/F_m of phytoplankton was relatively high (0.46) with little variation either between stations in the PIB (Fig. 6F) or over the top 50 m of the water column (Fig. 5F).

Table 3
Mean and standard deviation of biomass and nutrients in surface waters (10 m) of the glacier sites, Pine Island Bay, Pine Island Polynya, Amundsen Polynya and sea ice stations. Means are significantly different at the $p<0.05$ level unless connected by the same letter.

	n	Chl a ($\mu g\ L^{-1}$)	POC ($\mu mol\ L^{-1}$)	C:N [mol:mol]	POC:Chl a [wt:wt]	$\overline{a}^*$ ($m^2\ mg^{-1}$ Chl a)	NO_3 ($\mu mol\ L^{-1}$)	PO_4 ($\mu mol\ L^{-1}$)	DFe ($nmol\ L^{-1}$)
Glacier	7	0.93^{c} (1.21)	8.03 (7.57)	7.8^{a} (2.4)	148.0^{a} (60.6)	0.0094^{a} (0.0044) ($n=3$)	28.34 (2.41)	1.91 (0.34)	0.62 (0.34)
Pine Island Bay	10	4.60^{a} (1.92)	41.83^{a} (11.7)	6.96^{b} (1.21)	140.3^{a} (57.1)	0.0142^{a} (0.0071)	9.96^{a} (2.18)	0.85^{a} (0.30)	0.13^{a} (0.06)
Pine Island Polynya	13	9.49 (4.45)	61.38 (21.05)	6.72^{abc} (1.14)	86.1^{bc} (24.1)	0.0099^{a} (0.0014)	6.88^{a} (6.47)	0.75^{a} (0.30)	0.10^{a} (0.03)
Amundsen Polynya	5	4.33^{ab} (3.13)	38.2^{ab} (10.1)	6.16^{abc} (0.50)	219.2^{ac} (217.3)	0.0114^{a} (0.0050)	9.07^{a} (5.84)	0.80^{a} (0.38)	0.09^{a} (0.2)
Sea ice	15	3.22^{bc} (2.95)	22.54^{b} (17.89)	6.08^{c} (0.65)	109.2^{b} (40.3)	0.0141^{a} (0.0059)	18.80 (7.70)	1.27 (0.49)	0.13^{a} (0.09)

Table 4
Mean and standard deviation of phytoplankton community composition and F_v/F_m in surface waters (10 m) of the glacier sites, Pine Island Bay, Pine Island Polynya, Amundsen Polynya, and sea ice stations. Means are significantly different at the $p<0.05$ level unless connected by the same letter.

	n	*Diatoms* (*fraction of Chl a*)	*Phaeocystis antarctica* (*fraction of Chl a*)	*Green algae* (*fraction of Chl a*)	*Cryptophytes* (*fraction of Chl a*)	*Fe-limited P. antarctica* (*fraction of P. antarctica*)	F_v/F_m
Glacier	3	0.56^{a} (0.24)	0.44^{a} (0.24)	0.00^{a} (0.00)	0.00^{a} (0.00)	0.67^{abcd} (0.58)	0.52^{ac} (0.06) ($n=7$)
Pine Island Bay	10	0.08^{b} (0.05)	0.92^{b} (0.05)	0.00^{a} (0.00)	0.00^{a} (0.00)	0.48^{be} (0.16)	0.46^{bd} (0.03)
Pine Island Polynya	13	0.16^{bc} (0.13)	0.83^{b} (0.14)	0.01^{a} (0.01)	0.00^{a} (0.00)	0.90^{c} (0.11)	0.41^{e} (0.06)
Amundsen Polynya	5	0.32^{acd} (0.13)	0.67^{c} (0.13)	0.00^{a} (0.00)	0.00^{a} (0.00)	0.91^{acd} (0.18)	0.47^{cdef} (0.06)
Sea ice	9	0.44^{ad} (0.25)	0.48^{ac} (0.28)	0.06^{a} (0.08)	0.01^{a} (0.02)	0.60^{de} (0–0.43)	0.47^{abf} (0.07)

3.2.3. Pine Island Polynya

The mean salinity of surface waters in the PIP was slightly lower than that of the PIB (Table 2), particularly at stations further north, likely the result of sea ice melt (Fig. 4D). Surface temperatures were relatively high in the PIP, especially in the upper 10 m of the water column (Fig. 3A). The PIP was both salinity- and thermally-stratified, which resulted in a relatively shallow z_{UML} (mean 15.2 m). Like in the PIB, z_{UML} was shallower than z_c at all stations. The positive effect of this shallow z_{UML} on the E_{UML} was, however, offset by the high values of K_d (Table 2), resulting in an E_{UML} of 13.1 mol quanta $m^{-2}\ d^{-1}$, similar to that of the PIB.

Phytoplankton biomass was high in surface waters (10 m) of the PIP, with mean Chl a concentrations of 9.49 $\mu g\ L^{-1}$ and POC as high as 61.38 $\mu mol\ L^{-1}$ (Table 3). Mean surface Chl a was twice that of the PIB. We observed little temporal change in surface phytoplankton biomass in the PIP, with Chl a concentrations exceeding 10 $\mu g\ L^{-1}$ on both 15 January (Sta. 12 and 13) and on 30–31 January (Sta. 105, 106, and 107; Fig. 3F). These high Chl a concentrations were restricted to the upper 10 m of the water column (Fig. 3F).

The surface (10 m) concentration of DFe was generally low at stations north of Sta. 104 (<0.06 nM) and higher to the south (>0.11 nM) (Fig. 4E). Surface concentrations of NO_3 and PO_4 were somewhat variable between stations, with mean concentrations of 6.88 and 0.75 $\mu mol\ L^{-1}$, respectively (Table 3). Almost complete drawdown of NO_3 was observed at the mid-polynya stations 107 and 108 (0.21 and 0.32 μM respectively, Figs. 3B and 4B). These stations also had a relatively shallow z_{UML} (<10 m, Fig. 4C). A slight decrease in salinity at these stations indicated the influence of sea ice melt water.

The phytoplankton community in the surface waters of the PIP was dominated by *P. antarctica*, comprising on average 83% of Chl a biomass (Fig. 6A, Table 4). The mean contribution of diatoms to the surface phytoplankton community was 16%, which was double that of the PIB (Table 4). The highest contribution of diatoms to the surface phytoplankton community of the PIP was 46% at Sta. 14 in the south of the PIP. At some stations, the diatom contribution to the phytoplankton community in deep (100 m) waters was high (e.g. 69% at Sta. 105, Fig. 5B). The low Fe pigment signature of *P. antarctica* comprised an average of 90% of the *P. antarctica* community in surface waters (Table 4, Fig. 6E). The distribution of the high Fe and low Fe pigment signature was constant over the top 50 m of the water column, whereas the contribution of the low Fe pigment signature was somewhat lower at 100 m (Fig. 5E). Pigments of green algae or cryptophytes were not detected in the PIP.

The F_v/F_m of the phytoplankton was relatively low and exhibited little variation between stations within the PIP (mean 0.41; Fig. 6F). The one exception was Sta. 14 where the phytoplankton F_v/F_m was 0.55. The phytoplankton F_v/F_m in surface waters was lower than that below the z_{UML} (Fig. 5F).

Photosynthetic rates in surface waters of all stations in the PIP were high, with a mean P_m^* of 3.24 g C g^{-1} Chl $a\ h^{-1}$ and relatively little variation between stations (Table 5). The range of α^* in the PIP was similarly narrow, varying between 0.037 and 0.047 g C g^{-1} Chl $a\ h^{-1}$ ($\mu mol\ quanta\ m^{-2}\ s^{-1}$)$^{-1}$. Values for E_k ranged between 64 and 104 $\mu mol\ quanta\ m^{-2}\ s^{-1}$ at all stations. The QY was similar in most stations, varying between 0.074 and 0.107 mol C mol $quanta^{-1}$, but much lower in Sta. 129 (0.032 mol C mol $quanta^{-1}$).

3.2.4. Amundsen Polynya

We sampled only five stations in the AP between 1–12 February. The variability in most hydrographic parameters between these stations was relatively high. Low surface temperatures and low salinity indicated sea ice melt water influence in surface waters throughout the AP (Table 1, Fig. 3A and D). The mean z_{UML} was deeper than in other regions, mostly due to the uncharacteristically deep z_{UML} of 83 m at Sta. 114, which was well below the z_c. At other stations, the z_{UML} was >19 m (Table 2, Fig. 3C), and shallower than the z_c. This deep z_{UML}, combined with the lower solar angle later in the season, resulted in relatively low E_{UML}, although the difference in E_{UML} between the AP and the PIB and PIP was not statistically significant due to the large variability between stations.

The mean surface Chl a concentration in the AP was similar to that of PIB and thus lower than in the PIP (Table 3). Surface (10 m)

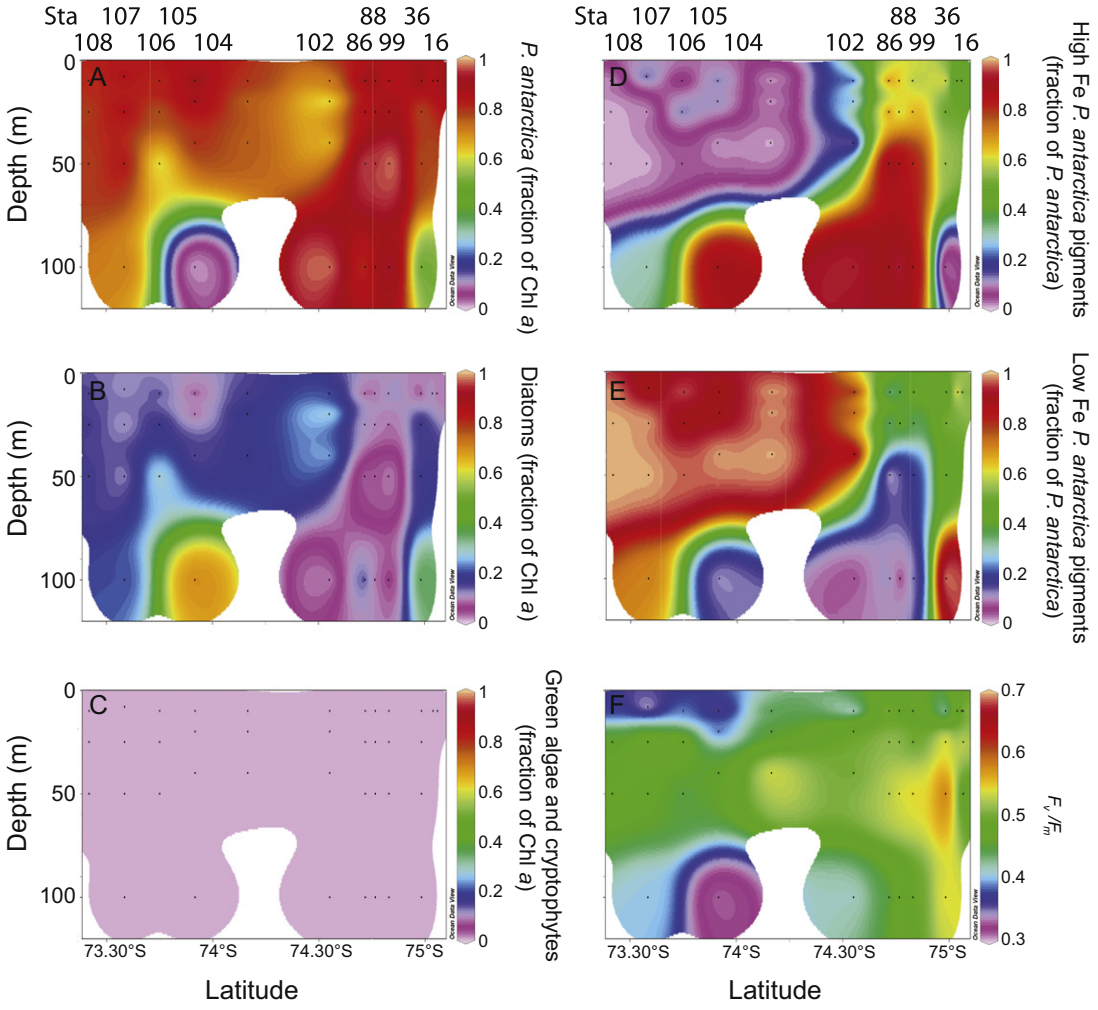

Fig. 5. Phytoplankton composition based on pigment analysis of the stations on a transect from the southwestern end of the PIG (Sta 16) to the northwest, transecting the PIB and the PIP (Sta 104–108). (A) Fraction of Chl *a* as *Phaeocystis antarctica*, (B) fraction of Chl *a* as diatoms, (C) fraction of Chl *a* as green algae and Cryptophytes, (D) fraction of *P. antarctica* with a high Fe pigment signature, (E) fraction of *P. antarctica* with a low Fe pigment signature, and (F) maximum photochemical efficiency of photosystem II (F_v/F_m).

concentrations of DFe were relatively low (Fig. 4E, Table 2), whereas the mean concentrations of NO_3 and PO_4 were similar to those of PIB, although the variability between stations was much greater in the AP.

The phytoplankton community in the AP was dominated by *P. antarctica* at three stations (Sta. 113, 118, and 153) and a mix between diatoms and *P. antarctica* in the two other stations (Sta. 114 and 148, Fig. 6A, B). The *P. antarctica* community at all depths was dominated by the low-Fe pigment signature (Fig. 6E). The mean F_v/F_m of surface phytoplankton in the AP was 0.47, similar to that of PIB (Table 4), but higher than in the PIP, and exhibited considerable variation between stations (Fig. 6F).

The mean P_m^* in the AP was high at 3.45 g C g^{-1} Chl *a* h^{-1} and similar to that of the PIP (Table 5). However, the mean α^* was 0.086 g C g^{-1} Chl *a* h^{-1} (μmol quanta m^{-2} s^{-1})$^{-1}$, almost twice as high as in the PIP. These parameters resulted in a mean E_k of 57 μmol quanta m^{-2} s^{-1}, which was lower than the PIP, although the difference was not statistically significant due to the low number of stations that were sampled. The mean QY of phytoplankton in the AP was 0.168 mol C mol quanta^{-1} and thus higher than that of the PIP.

3.2.5. Sea ice stations

A band of sea ice bordered the north of the Pine Island and Amundsen polynyas (Fig. 1). In addition, an area with both sea ice and icebergs extended to the north of the Thwaites Glacier tongue in between the PIP and the AP. The temperature and salinity of surface waters at sea ice stations were lower than elsewhere (Table 2, Figs. 2, 4A and B), indicating a clear influence of sea ice melt water. This additional melt water induced stable water columns with a mean z_{UML} of 15.7 m, although three stations on the northern end of the ice showed slightly deeper z_{UML} of >20 m (Fig. 4C). The z_{UML} was always shallower than the z_c. E_{UML} in the sea ice zone was similar to other regions (Table 2), with the positive effects of low K_d offsetting the negative effects of ice cover.

Biomass in the water column in the sea ice region was highly variable, but generally low (<3.5 μg Chl *a* L^{-1}) in waters at the northern end of the ice and high at the southern end, near the edge of the polynya (>5.0 μg Chl *a* L^{-1}, Fig. 4F). In general, the surface (10 m) concentrations of DFe were moderately low (mean 0.13 nmol L^{-1}), whereas surface concentrations of NO_3 and PO_4 were relatively high (mean 18.80 and 1.27 μmol L^{-1}, respectively) (Fig. 4B, Table 3). In one sea ice station (Sta. 111), NO_3 was drawn down to only 0.73 μmol L^{-1} (0.75 μmol L^{-1} after salinity correction).

The phytoplankton community in surface waters of sea ice stations was primarily a mix of *P. antarctica* and diatoms (Table 4, Fig. 6 A and B), although green algae and cryptophytes were also present in some ice stations, occasionally making up $>20\%$ of the community (Sta. 5 and 131, Fig. 6C). In general, the contribution of diatoms was higher at the northern end of the region, whereas

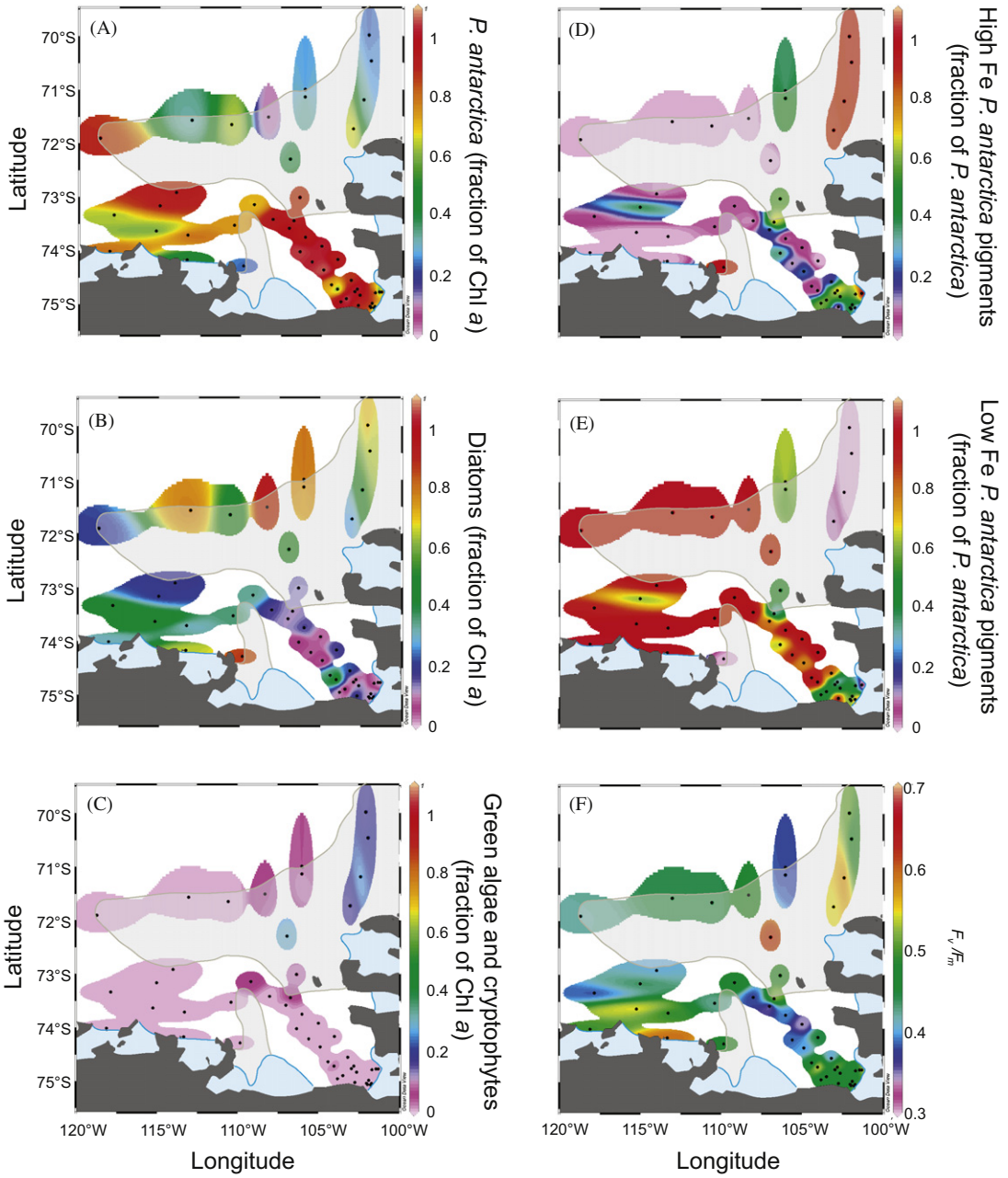

Fig. 6. Phytoplankton composition based on pigment analysis of surface waters (10 m) of the Amundsen Sea with the >50% sea ice concentration shaded in gray. Ice shelves are light blue whereas land is gray. (A) Fraction of Chl *a* as *Phaeocystis antarctica*, (B) fraction of Chl *a* as diatoms, (C) fraction of Chl *a* as green algae and Cryptophytes, (D) fraction of *P. antarctica* with high a Fe pigment signature, (E) fraction of *P. antarctica* with a low Fe pigment signature, and (F) F_v/F_m. (For interpretation of the references to color in this figure legend, the reader is referred to the web version of this article.)

P. antarctica dominated the polynya edges. The exception was station 158, the most western station at the northern ice edge, that was dominated by *P. antarctica* (Fig. 6A and B). We sampled this station on 14 February when the ice on the western end of the AP was disappearing. This may have allowed northward advection of surface waters from the polynya containing *P. antarctica*. The F_v/F_m of surface phytoplankton was highly variable in the ice stations, varying between 0.37 and 0.63, the highest value we recorded (Fig. 6F).

Both the P_m^* (3.13 g C g^{-1} Chl *a* h^{-1}) and α^* (0.042 g C g^{-1} Chl *a* h^{-1} [μmol quanta m^{-2} s^{-1}]$^{-1}$) showed more variability in the ice stations than in the polynya stations and did not differ significantly from values in either polynya. Similarly, the E_k values resembled those in the polynyas (mean 78 μmol quanta m^{-2} s^{-1}). The QY was relatively uniform in all stations, with a mean of 0.067 mol C mol quanta^{-1} (Table 5).

3.3. Depth integrated Chl a and primary production

Phytoplankton standing crop in the upper 200 m of the water column was generally low in the upwelling waters associated with glacier stations and increased northward until reaching a biomass maximum (~700 mg Chl *a* m^{-2}) in the polynyas (Table 6, Fig. 7A). Despite the higher surface Chl *a* concentrations in the PIP, depth-integrated Chl *a* was similar to that in PIB and the AP (Table 6, Fig. 7A), since the deeper z_{UML} in the PIB and AP resulted in higher Chl *a* values at depth, thereby offsetting the higher surface Chl *a* concentrations in the PIP. Depth-integrated

Table 5
Mean and standard deviation of phytoplankton photosynthesis versus irradiance relationships in surface waters (10 m) of the Pine Island Polynya, Amundsen Polynya, and sea ice stations. Means are significantly different at the $p < 0.05$ level unless connected by the same letter.

	n	P_m^* (g C g^{-1} Chl *a* h^{-1})	α^* (g C g^{-1} Chl *a* h^{-1} [μmol quanta m^{-2} s^{-1}]$^{-1}$)	E_k (μmol quanta m^{-2} s^{-1})	P_0^* (g C g^{-1} Chl *a* h^{-1})	*QY* (mol C mol quanta^{-1})
Glacier	0	ND	ND	ND	ND	ND
Pine Island Bay	0	ND	ND	ND	ND	ND
Pine Island Polynya	6	3.24[a] (0.50)	0.042[a] (0.004)	78[a] (14)	0.03[a] (0.11)	0.077[a] (0.025)
Amundsen Polynya	5	3.45[a] (0.67)	0.086[a] (0.055)	56[a] (23)	−0.13[a] (0.13)	0.168 (0.048)
Sea ice	9	3.13[a] (0.87)	0.042[a] (0.012)	78[a] (21)	−0.25[a] (0.46)	0.067[a] (0.015)

Table 6
ΣChl *a* of the top 200 m of the water column, net community NO_3 uptake, new productivition based on NO_3 uptake, and N-export in the upper 100 m of the water column, and *PE* data in surface waters (10 m) of the glacier sites, Pine Island Bay, Pine Island Polynya, Amundsen Polynya, and sea ice stations. Means are significantly different at the $p < 0.05$ level unless connected by the same letter.

	n	Σ *Chl a* (mg m^{-2})	*NO_3 uptake* (mol m^{-2})	*N-export* (mol m^{-2})	*New production since December* 1st (g C m^{-2} d^{-1})	*n*	*Water column productivity* (g C m^{-2} d^{-1})
Glacier	9	75[a] (106)	0.13 (0.20)	0.09 (0.15)	0.22[a] (0.28)	0	ND
Pine Island Bay	7	412[b] (202)	1.24[a] (0.13)	0.90[a] (0.10)	1.44[b] (0.24)	10	2.59[da] (0.88)
Pine Island Polynya	10	560[b] (207)	1.17[a] (0.19)	0.74 (0.11)	1.26[b] (0.22)	6	4.18[b] (1.50)
Amundsen Polynya	4	328[b] (253)	1.23[a] (0.22)	1.07[a] (0.29)	0.99 (0.10)	5	2.44[ab] (1.47)
Sea ice	12	164[a] (147)	0.52 (0.31)	0.36 (0.23)	0.47[a] (0.28)	9	1.56[a] (1.48)

[d] Mean *PE* parameters from the PIP and AP stations were used to compute the water column productivity in the PIB.

Chl *a* in the sea ice zone was lower than in the polynyas, with the highest biomass located at the southern and western ice edge.

Depth-integrated water column primary production, calculated from measured phytoplankton biomass, light distribution, and *P–E* relationships (Fig. 7D, Table 6) was higher in the PIP (mean 4.18 g C m^{-2} d^{-1}) than in the PIB and AP (mean 2.58 and 2.44 g C m^{-2} d^{-1}, respectively), due mainly to the high phytoplankton biomass at the surface where ample light was available for photosynthesis. Primary production in the sea ice zone was much more variable than in the polynyas, with rates as high as 4.9 g C m^{-2} d^{-1} (Sta. 111) and 2.2 g C m^{-2} d^{-1} (Sta. 127), but generally < 1.9 g C m^{-2} d^{-1}.

New production since 1 December (Table 6, Fig. 7C) was very low in most glacier stations, although small NO_3 deficits were apparent in Sta. 17 and 81. In the PIB and PIP the NO_3 deficits were large, resulting in new production rates of 1.44 and 1.26 g C m^{-2} d^{-1} since Dec 1, respectively. The NO_3 deficit in the AP was similar to that of the PIB and PIP, which resulted in lower rates of new production, since the AP was sampled later in the season. The similarity in new production between the PIB and PIP contrasts the higher mean water column productivity in the PIP based on ^{14}C-uptake. This difference may be explained by the different dates of opening of the two polynyas. As shown in Fig. 7F, the PIB was mostly ice-free on 1 December, whereas approximately half of the PIP was still covered with ice, thereby reducing light availability and productivity in the PIP early in the season. During the growing season, higher mean water column productivity rates in the PIP likely made up for the reduction in productivity early in the season.

NO_3 uptake and new production were highly variable in the sea ice zone, exhibiting lower rates than in the polynyas (mean 0.52 mol m^{-2} and 0.47 g C m^{-2} d^{-1}, respectively). New production was lowest at stations that where sampled early in the season northeast of the sea ice edge (Sta. 2, 3, and 7). The highest values were measured at the southern ice edge, in stations bordering the PIP (Sta. 11) and AP (Sta. 111, 127; Fig. 7B), resulting in new production rates of 0.88, 0.85 and 0.91 g C m^{-2} d^{-1}, respectively. NO_3 drawdown at these stations was similar to that in the polynyas.

Estimates of N-export followed the trends in NO_3 deficits (Table 6, Fig. 7E), being very low at the glacier stations (mean 0.09 mol N m^{-2}) and highest in PIB and the AP (mean 0.90 and 1.07 mol N m^{-2}, respectively). It should be noted, however, that the AP was sampled almost two weeks later than the PIB. Surprisingly, N-export in the PIP was lower (mean 0.74 mol N m^{-2}) than in both PIB and the AP. N-export at the sea ice stations was variable (mean 0.36 mol N m^{-2}), with the highest values found at stations that were adjacent to the AP and sampled later in the season (Sta. 111 and 127).

4. Discussion

4.1. Impact of glacial Fe input on phytoplankton blooms in the Amundsen Sea

A massive phytoplankton bloom dominated by *P. antarctica* was responsible for high primary productivity in the Amundsen Sea, most notably in the PIP. The mean surface concentrations of Chl *a* we observed in the PIP were similar to those observed during exceptionally large phytoplankton blooms in other productive polynya systems such as the Ross Sea (Smith et al., 2006) and approximately two-fold higher than mean surface Chl *a* concentrations for the Ross Sea (Smith et al., 2010). The high phytoplankton biomass and productivity resulted in near depletion of NO_3 in surface waters in the PIP and in some sea ice stations, which has only been reported in exceptionally large phytoplankton blooms in the WAP region (Ducklow et al., 2007) and only very rarely in the Ross Sea (Fitzwater et al., 2000). Moreover, the high phytoplankton biomass in surface waters, especially in the PIP, resulted in high levels of water column productivity, exceeding 3 g C m^{-2} d^{-1}. These values exceeded those measured during peaks in phytoplankton blooms in the WAP of 1.8 g C m^{-2} d^{-1} (Vernet et al., 2008) and the Ross Sea 2.1 g C m^{-2} d^{-1} (Arrigo et al., 2000, 2008b).

Gerringa et al. (2012) showed that Fe released from the PIG is the main source of DFe for the phytoplankton bloom in both PIB and the PIP. The high concentrations of DFe in meltwater MCDW

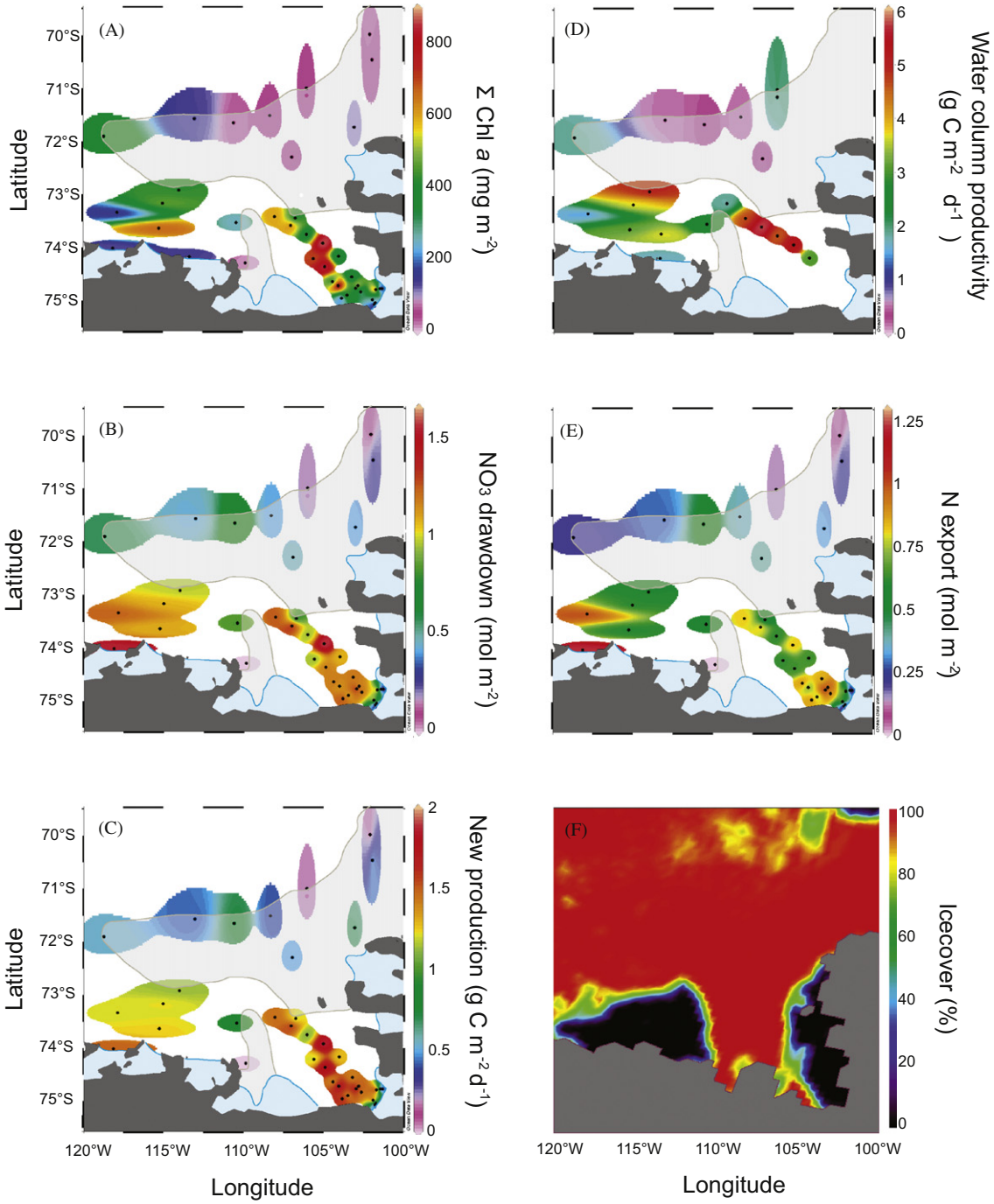

Fig. 7. Depth-integrated properties of the Amundsen Sea with the >50% sea ice concentration shaded in gray. Ice shelves are light blue whereas land is gray. (A) Depth-integrated Chl *a*, (B) NO_3 uptake in the upper 100 m, (C) new production in the upper 100 m, (D) water column productivity, (E) N-export out of the upper 100 m, and (F) and ice cover on 1 December 2008. (For interpretation of the references to color in this figure legend, the reader is referred to the web version of this article.)

from the PIG showed an exponential decline with distance from the PIG, resembling a dilution process from a single source. This distribution was used for lateral DFe flux calculations in surface waters, revealing that the lateral DFe flux from the PIG could satisfy the total calculated Fe demand of the *P. antarctica* bloom at a distance of 150 km, at the southern end of the PIP. Similarly, high concentrations of DFe were observed in waters close to the Dotson and Crosson ice shelves in the AP (Gerringa et al., 2012). The exponential DFe decrease with distance from the glacier was higher in surface waters with phytoplankton than at depth where no phytoplankton was present, reflecting Fe uptake during the developing phytoplankton bloom.

The decrease in DFe in surface waters between PIG and the PIP was mirrored by changes in the relative abundance of *P. antarctica* that were acclimated to high Fe, as determined by their pigment signature. *P. antarctica* with the high Fe pigment signature dominated the phytoplankton community in PIB, which was characterized by its higher DFe concentrations in surface waters. Conversely, *P. antarctica* with a low-Fe pigment signature dominated the PIP where DFe concentrations were lower. Moreover, high-Fe acclimated *P. antarctica* in PIB exhibited markedly elevated values for F_v/F_m that often exceeded 0.5 and approximated those of nutrient-replete *P. antarctica* cultures (Van Leeuwe and Stefels, 2007, Kropuenske et al., 2009, Alderkamp et al., 2012).

In contrast, values of F_v/F_m for low-Fe acclimated *P. antarctica* growing in the PIP were lower, consistent with previous observations by Wright et al. (2010). There were no temporal trends in high Fe and low Fe *P. antarctica* signature, nor in phytoplankton *Fv/Fm*, in either the PIB or the PIP over the course of our study. This lack of temporal change confirms phytoplankton responded to a constant flux of DFe from the PIG into the PIB and PIP (Gerringa et al., 2012), rather than depletion of the winter stock over the course of the growing season. Unfortunately the more complex hydrography in the AP and areas of sea ice cover make it difficult to discern whether similar relationships between DFe and *P. antarctica* pigment signature existed there.

Interestingly, despite the fact that the PIP was characterized by low DFe concentrations, reduced F_v/F_m, and dominance by low-Fe acclimated *P. antarctica*, the addition of exogenous Fe to these waters during bioassay experiments had no impact on phytoplankton biomass (Mills et al., 2012), suggesting that low Fe concentrations are not limiting phytoplankton growth in the PIP. Therefore, while physiological acclimation of *P. antarctica* to low Fe conditions was apparent in the PIP, DFe concentrations were not low enough to limit the growth of *P. antarctica*. Recently, culture studies under Fe-limitation revealed that *P. antarctica* is capable of maintaining high rates of P_m^* (Alderkamp et al., 2012) that were similar to values measured here in the PIP and higher than those reported for *P. antarctica*-dominated blooms in the Ross Sea (Van Hilst and Smith, 2002; Shields and Smith, 2009). Thus, the photosynthetic architecture of *P. antarctica* seems capable of maintaining high photosynthetic rates under low DFe concentrations. Consequently, while the low-Fe pigment signature of *P. antarctica* is indicative of acclimation to low Fe concentrations (DiTullio et al., 2007; Van Leeuwe and Stefels, 2007; Alderkamp et al., 2012; Mills et al., 2012), it is not indicative of reduced *P. antarctica* growth rates in waters with low Fe concentration and should not be considered a reliable proxy for Fe-limitation of phytoplankton productivity.

The in situ observations of high phytoplankton biomass and productivity corroborate those made by satellite (Arrigo and Van Dijken, 2003; Arrigo et al., 2012). The satellite observations and productivity algorithms showed primary productivity of the 2008–09 season in the Pine Island Polynya exceeded the 13-year annual mean by 38%, whereas the Amundsen Polynya was 16% higher. Several years within the 1997–2010 period showed a similarly high or higher annual productivity, thus, whereas 2008–09 was a productive year, it was not exceptionally high (Arrigo et al., 2012). This suggests that the Fe flux from the PIG and other glaciers flowing into the Amundsen Sea support highly productive phytoplankton blooms on a regular basis.

4.2. Effects of light availability on phytoplankton productivity in the Amundsen Sea

Light plays a prominent role in controlling Antarctic phytoplankton abundance and productivity (De Baar et al., 2005), which will be especially pertinent throughout much of the Amundsen Sea shelf, where DFe was not limiting phytoplankton productivity. The E_{UML} depends on incident irradiance, sea ice cover, z_{UML}, and water optical properties. Vertical water column stability is increased (z_{UML} decreases) by surface freshening due to ice melt and warming from solar energy input and decreased by wind-induced vertical mixing (z_{UML} increases). During our voyage, the balance between these factors controlling light availability differed markedly in the PIB and PIP.

The z_{UML} of the PIB was deeper than that of the PIP, and since there was no vertical structure in salinity, stratification in the PIB was weaker than in the PIP, where influence of sea ice melt resulted in fresher surface waters. The surface salinity of PIB stations showed no signs of freshening when compared to the MCDW flowing out from under the PIG, indicating that stratification was solely due to surface warming. This suggests that the loss of sea ice cover from the PIB was due to advection, presumably driven by surface katabatic winds, rather than by melting in place. These katabatic winds would have advected the sea ice from the PIB into the PIP, which was still approximately 50% ice covered on 1 December. Katabatic winds can deeply mix surface waters, thereby lowering the E_{UML} early in the season and potentially delaying bloom development, as was observed in the Ross Sea Polynya (Arrigo et al., 1998). Accordingly, satellite data revealed that the phytoplankton blooms in the waters encompassing the PIB and PIP are delayed by an average of 30 days relative to the opening of the polynyas (Arrigo et al., 2012). The frequency of katabatic winds generally diminishes in austral spring, thus allowing surface waters of PIB to thermally stratify which increases the E_{UML} and promotes phytoplankton bloom development.

In contrast, lower surface salinity in the PIP suggests that sea ice melt plays a larger role in surface water stratification, producing a shallow UML that is both salinity and temperature stratified. Because of the stronger stratification in the PIP, the input of wind energy during the growing season resulted in a shallower z_{UML} and higher E_{UML}. Physiological properties of the *P. antarctica* communities in the PIP showed responses to the higher light availability in the PIP when compared to the PIB. *P. antarctica* in the PIP exhibited higher POC/Chl *a* ratios than in the PIB, consistent with acclimation to higher growth irradiance (Arrigo et al., 2010). The POC/Chl *a* ratio was not affected by Fe-limitation (Alderkamp et al., 2012), thus DFe concentrations will not affect the difference in POC/Chl *a* ratio between the PIB and PIP. The shallower UML and higher E_{UML} resulted in enhanced phytoplankton biomass and a higher degree of nutrient depletion in surface waters of the PIP, despite its waters becoming ice-free later in the spring.

4.3. Phytoplankton productivity in the Amundsen Sea compared to the Ross Sea

Satellite studies have revealed that the Ross and Amundsen Sea harbor the most productive polynyas in the Southern Ocean, with summer area of the Ross Sea area ten times as big as the PIP (Arrigo and Van Dijken, 2003; Arrigo et al., 2008a, b). The high phytoplankton biomass and water column productivity rates we observed in the Amundsen Sea confirmed the high net productivity, however, new production rates based on NO_3 removal in the PIB, PIP, and AP were only approximately half of what was reported in a high productivity year for the Ross Sea, and similar to the mean new production over four years (Arrigo et al., 2000; Smith et al., 2006, 2011). One explanation for the relatively low depth-integrated NO_3-removal associated with the high phytoplankton biomass in the Amundsen Sea may be that the highest Chl *a* and lowest NO_3 concentrations were largely restricted to the top 10 m of the water column. In contrast, high Chl *a* concentrations and substantial NO_3 removal were reported down to 40 m depth in the Ross Sea (Arrigo et al., 2000; Fitzwater et al., 2000; Smith et al., 2006), resulting in higher new production integrated over the water column. In addition, the bloom in the Ross Sea usually starts in early November (Arrigo and Van Dijken, 2003; Smith et al., 2006, 2011) and thus much earlier than the blooms in the PIP and AP that start in early December (Arrigo and Van Dijken, 2003; Arrigo et al., 2012). The demise of the blooms in the regions is timed similarly in late February (Arrigo and Van Dijken, 2003), resulting in a shorter bloom duration in the Amundsen Sea when compared to the Ross Sea. However, even on a daily basis starting from 1 November, the daily new production in the Ross Sea in high bloom years was substantially higher than what we measured in the PIB, PIP, and AP (Smith et al., 2006, 2011). Our

estimate of new production assumes no input of new NO_3 in the upper water column. Clearly, there was outflow of MCDW with a mean NO_3 concentration of 28.34 μmol L^{-1} to the upper water column in several glacier sites, which may have lead to underestimation of biological NO_3-removal and new production, especially in the PIB that saw inflow of MCDW from under the PIG.

Remarkably, new production in the PIB was slightly higher than in the PIP, despite reports of northward advection of surface waters from the PIB into the PIP (Hellmer et al., 1998). This advection would bring waters containing a phytoplankton bloom that had already drawn down NO_3 from the PIB into the PIP, resulting in an overestimation of NO_3 uptake in the PIP. However, the slightly lower NO_3 uptake measured in the PIP suggests that the amount of water advecting from the PIB to the PIP is relatively small.

The N-export we estimated in the polynyas resembled the mean over four seasons that was measured in the Ross Sea, and was substantially lower than what was measured in a high bloom year (Smith et al., 2006, 2011), both expressed on a daily basis with an earlier starting date in the Ross Sea, and expressed on an annual basis. The fraction of NO_3 uptake that was exported ranged from 32% to 68% in polynya waters of the Amundsen Sea, which was within the range of ratios reported for annual fraction of NO_3 uptake in the Ross Sea (Smith et al., 2011). The Ross Sea showed a high degree of interannual variation, both in productivity and export, and also in the coupling between these, when estimated from NO_3 or silicate drawdown or derived form sediment traps (Smith et al., 2011). Future studies will provide information on interannual variation in productivity and export in waters of the Amundsen Sea.

4.4. Spatial distributions of *P. antarctica* and diatoms in the Amundsen Sea

Phytoplankton blooms were dominated by *P. antarctica* in the PIB and PIP, whereas pre-(December) and post-bloom (March) polynya communities were reported to be dominated by diatoms or a mix of diatoms and *P. antarctica* in earlier seasons (Fragoso and Smith, 2012). During our study, diatoms and a mix of *P. antarctica* and diatoms were associated with waters that had substantial sea ice cover. A similar pattern of *P. antarctica* dominating polynya blooms and diatoms dominating the marginal ice zone was described previously in the Ross Sea (Arrigo et al., 1999; Smith et al., 2010). Several hypotheses have been put forward to explain this pattern, including (1) increased seeding of the MIZ phytoplankton bloom by diatoms released from melting sea ice (Smith and Nelson, 1986; Leventer, 2003; Arrigo et al., 2000; Mangoni et al., 2009), (2) diatoms outcompeting *P. antarctica* at high Fe concentrations near the MIZ (Sedwick et al., 1997), (3) a superior ability for diatoms to access ligand-bound Fe in areas of sea ice melt, a mechanism put forward in the modeling study of Tagliabue and Arrigo (2005), and (4) *P. antarctica* outcompeting diatoms under light conditions with variable light levels mimicking rapid vertical mixing in the upper water column (Arrigo et al., 2003, 2010, Kropuenske et al., 2009, Mills et al., 2010).

Seeding of the water column by sea ice diatoms did not appear to affect phytoplankton community composition in the Amundsen Sea during our study, since *P. antarctica* dominated blooms in both PIB, which exhibited little evidence of sea ice melt, and the PIP, where input of sea ice melt water was substantial. Furthermore, because both diatoms and *P. antarctica* have been observed growing in pack ice (Arrigo et al., 2003; Tison et al., 2010), melting sea ice could have inoculated the upper water column with either taxa. Similarly, spatial differences in Fe concentration are unlikely to have affected the competitive outcome between *P. antarctica* and diatoms, since *P. antarctica* dominated both PIB, where Fe input from the PIG was high, and the PIP, which had much lower rates of Fe input and DFe concentrations in surface waters (Gerringa et al., 2012). In the same way, concentrations and characteristics of Fe-binding dissolved organic ligands differed from the PIB to the PIP (Thuróczy et al., 2012). The outflowing MCDW from under the PIG contained ligands with a relatively low conditional stability constant (K'). The K' of ligands in the PIB was similar to that of the MCDW, however, in the PIP ligands with a markedly higher K' were measured. Moreover, the concentration of excess ligands that were not bound by DFe increased with distance from the PIG, suggesting that organic material produced during the *P. antarctica* bloom was changing the ligand composition (Thuróczy et al., 2012). Furthermore, addition of different organic model Fe-binding ligands did not affect the relative abundance of diatoms and *P. antarctica* in bioassay experiments (Mills et al., 2012).

The differences in light conditions associated with spatial differences in upper ocean stratification seem to best explain the distribution of *P. antarctica* and diatoms in the Amundsen Sea, since *P. antarctica* dominated surface waters with a more variable light environment and diatoms dominating regions with less fluctuations in light. In both the PIB and PIP, the z_{UML} was mostly below z_{EU}, thus, vertical mixing below the euphotic zone created highly variable light levels. Even in the PIP, where the z_{UML} was shallower than in the PIB and in the *P. antarctica* dominated Ross Sea Polynya (Arrigo et al., 1999, Fragoso and Smith, 2012), mixing was below the z_{EU} due to the high K_d resulting from the high phytoplankton biomass. Although we do not know the z_{UML} early in the season during bloom development, z_{UML} was at or below z_{EU} during the first transect of PIP on 15 January just before the peak of the phytoplankton biomass, as well as during the second transect on 31 January, just before the phytoplankton bloom started to decline. Since the wind speeds were moderate during the NBP 09-01 cruise, wind-driven vertical mixing in the UML resulted in a dynamic irradiance climate where periods of high light when phytoplankton are mixed up to the surface were interchanged with periods in the dark when they are mixed below the z_{EU}. Culture studies have shown that *P. antarcica* is well adapted to these large fluctuations in irradiance (Kropuenske et al., 2009, Mills et al., 2010), particularly under low Fe conditions (Alderkamp et al., 2012), such as those we observed in the PIP. In contrast, the z_{UML} at sea ice stations dominated by diatoms was always above the z_{EU}, thus providing a more stable light climate in which diatoms thrive (Kropuenske et al., 2009, Mills et al., 2010). Remarkably, the mean E_{UML} did not differ between sea ice stations and polynya stations, indicating that it was the degree of fluctuation, not the absolute light levels, that controlled *P. antarctica* and diatom distributions.

4.5. Antarctic wide effects of input of glacial DFe on phytoplankton productivity

Many ice shelves on Antarctica are thinning as a result of acceleration of glaciers along the ice sheet margins (Pritchard et al., 2009). These melting glaciers are a significant source of Fe input into coastal polynyas (Raiswell et al., 2008; Gerringa et al., 2012). Because several rapidly thinning glaciers drain into the Amundsen Sea, the phytoplankton response in this region may provide insight about other coastal polynyas in the Antarctic region that are affected by thinning ice sheets, or will be in the future as a consequence of global warming. During the DynaLiFe project, we showed that DFe released from the PIG could sustain the phytoplankton bloom in PIB and the PIP. Ligands likely prevented aggregation of the glacier-derived DFe, and thus aided in keeping the glacier-derived DFe in solution in the upper water column (Thuróczy et al., 2012). Moreover, bioassay experiments

with several different organic model Fe-binding ligands showed that ligand-bound DFe was largely accessible to phytoplankton (Mills et al., 2012). This high Fe input resulted in a highly productive *P. antarctica* bloom that significantly reduced surface water pCO_2, making the Amundsen Sea polynyas a net sink for atmospheric CO_2 (Tortell et al., 2012).

The high phytoplankton productivity as a result of glacial input of DFe indicates that melting glaciers have the potential to increase CO_2 uptake by phytoplankton and thus act as a small negative feedback to anthropogenic CO_2 emissions. Other factors influencing the annual productivity in the polynyas were the time of polynya opening and the z_{UML}. If elevated temperatures lead to earlier polynya opening dates, this may increase future productivity of Antarctic polynyas by prolonging the phytoplankton growing season. Comparing the z_{UML} in the PIB and the PIP indicated that influence of glacial melt water in the PIB did not lead to stabilization of the water column that is favorable for a phytoplankton bloom to develop. The influence of sea ice melt in the PIP, however, did affect the z_{UML} favorably, resulting in the highest levels of surface biomass and water column productivity.

The phytoplankton blooms in the polynyas were dominated by colonial *P. antarctica*. The high biomass levels created a dynamic light regime with mixing below the z_{EU} that was favorable for *P. antarctica* (Kropuenske et al., 2009, Mills et al., 2010), even though the UML was relatively shallow, especially in the PIP. Since the calculated Fe demands of the *P. antarctica* bloom in the PIP required the input of glacial DFe to sustain these high biomass levels (Gerringa et al., 2012), the high biomass that resulted in a dynamic light climate in the shallow UML may be viewed as a mechanism by which glacier melt favors *P. antarctica* over diatoms. The dominance of *P. antarctica* may further increase the CO_2 drawdown when compared to diatom dominated systems, as it was shown in the Ross Sea that *P. antarctica* has a higher CO_2 drawdown per unit *P* than diatoms (Arrigo et al., 1999). In addition, *P. antarctica* is not preferentially grazed by the zooplankton and krill (Nejstgaard et al., 2007) that form the link between phytoplankton and upper trophic levels. Thus, *P. antarctica*-dominated systems are generally believed to result in less carbon being funneled towards higher trophic levels than diatom dominated systems (Schoemann et al., 2005). This may have a negative effect on higher organisms, such as penguins and whales that depend on polynyas for their food sources (Arrigo and Van Dijken, 2003, Ainley et al., 2006).

Acknowledgments

We thank the captain and crew of the RVIB *Nathaniel B. Palmer* as well as Raytheon staff for their support, and cruise leaders Stan Jacobs and Adrian Jenkins and all NBP 0901 participants for their help. Frank Nitsche is acknowledged making Fig. 1. This research was sponsored by the NSF DynaLiFe program (grant ANT-0732535 to KRA) in the framework of the US-IPY program and the Netherlands AntArctic Program (NAAP grant 851.20.041 to AGJB).

References

Ainley, D.G., Ballard, G., Dugger, K.M., 2006. Competition among penguins and cetaceans reveals trophic cascades in the western Ross Sea, Antarctica. Ecology 87, 2080–2093.

Alderkamp, A.C., Kulk, G., Buma, A.G.J., Visser, R.J.W., Van Dijken, G.L., Mills, M.M., Arrigo, K.R., 2012. The effect of iron limitation on the photophysiology of *Phaeocystis antarctica* and *Fragilariopsis cylindrus* under dynamic irradiance. J. Phycol. doi:10.1111/j.1529-8817.2011.01098.x.

Allison, I., Brandt, R.E., Warren, S.G., 1993. East Antarctica sea ice: albedo, thickness distribution, and snowcover. J. Geophys. Res. 98 (C7), 12417–12429.

Arrigo, K.R., DiTullio, G.R., Dunbar, R.B., Robinson, D.H., VanWoert, M., Worthen, D.L., Lizotte, M.P., 2000. Phytoplankton taxonomic variability in nutrient utilization and primary production in the Ross Sea. J. Geophys. Res.-Oceans 105, 8827–8845.

Arrigo, K.R., Mills, M.M., Kropuenske, L.R., Van Dijken, G.L., Alderkamp, A.-C., Robinson, D.H., 2010. Photophysiology in two major Southern Ocean taxa: photosynthesis and growth of *Phaeocystis antarctica* and *Fragilariopsis cylindrus* under different irradiance levels. Integrative and Comparative Biology 50, 950–966.

Arrigo, K.R., Robinson, D.H., Worthen, D.L., Dunbar, R.B., DiTullio, G.R., VanWoert, M., Lizotte, M.P., 1999. Phytoplankton community structure and the drawdown of nutrients and CO_2 in the Southern Ocean. Science 283, 365–367.

Arrigo, K.R., Van Dijken, G.L., Long, M.C., 2008a. Coastal Southern Ocean: a strong anthropogenic CO_2 sink. Geophysical Research Letters 35, L21602. http://dx.doi.org/:10.1029/2008GL035624.

Arrigo, K.R., Van Dijken, G.L., 2003. Phytoplankton dynamics within 37 Antarctic coastal polynya systems. J. Geophys. Res.-Oceans—Oceans 108 (C8), 3271. http://dx.doi.org/:10.1029/2002JC001739.

Arrigo, K.R., Van Dijken, G.L., Bushinsky, S., 2008b. Primary production in the Southern Ocean, 1997-2006. J. Geophys. Res.—Oceans 113, C08004. http://dx.doi.org/:10.1029/2007JC004551.

Arrigo, K.R., Worthen, D.L., Robinson, D.H., 2003. A coupled ocean-ecosystem model of the Ross Sea: 2. Iron regulation of phytoplankton taxonomic variability and primary production. J. Geophys. Res.—Oceans 108. http://dx.doi.org/:10.1029/2001JC000856.

Arrigo, K.R., Weiss, A.M., Smith, W.O., 1998. Physical forcing of phytoplankton dynamics in the southwestern Ross Sea. J. Geophys. Res.—Oceans 103, 1007–1021.

Arrigo, K.R., Lowry, K., Van Dijken, G.L., 2012. Annual changes in sea ice and phytoplankton in polynyas of the Amundsen Sea, Antarctica. Deep-Sea Res. II 71–76, 5–15.

Boyd, P.W., Jickells, T., Law, C.S., Blain, S., Boyle, E.A., Buesseler, K.O., Coale, K.H., Cullen, J.J., de Baar, H.J.W., Follows, M., Harvey, M., Lancelot, C., Levasseur, M., Owens, N.P.J., Pollard, R., Rivkin, R.B., Sarmiento, J., Schoemann, V., Smetacek, V., Takeda, S., Tsuda, A., Turner, S., Watson, A.J., 2007. Mesoscale iron enrichment experiments 1993–2005: Synthesis and future directions. Science 315, 612–617.

Bricaud, A., Stramski, D., 1990. Spectral absorption-coefficients of living phytoplankton and nonalgal biogenous matter—a comparison between the Peru upwelling area and the Sargasso Sea. Limnol. Oceanogr. 35, 562–582.

Buma, A.G.J., Debaar, H.J.W., Nolting, R.F., Vanbennekom, A.J., 1991. Metal enrichment experiments in the Weddell–Scotia seas—effects of iron and manganese on various plankton communities. Limnology and Oceanography 36, 1865–1878.

Caron, D.A., Dennett, M.R., Lonsdale, D.J., Moran, D.M., Shalapyonok, L., 2000. Microzooplankton herbivory in the Ross Sea, Antarctica. Deep-Sea Research II Topical Studies in Oceanography 47, 3249–3272.

Cisewski, B., Strass, V.H., Losch, M., Prandke, H., 2008. Mixed layer analysis of a mesoscale eddy in the Antarctic Polar Front Zone. J. Geophys. Res.-Oceans 113, C05017. http://dx.doi.org/:10.1029/2007JC004372.

Cullen, J.J., Davis, R.F., 2003. The blank can make a big difference in oceanographic measurements. Limnology and Oceanography Bulletin 12, 29–35.

De Baar, H.J.W., Boyd, P.W., Coale, K.H., Landry, M.R., Tsuda, A., Assmy, P., Bakker, D.C.E., Bozec, Y., Barber, R.T., Brzezinski, M.A., Buesseler, K.O., Boye, M., Croot, P.L., Gervais, F., Gorbunov, M.Y., Harrison, P.J., Hiscock, W.T., Laan, P., Lancelot, C., Law, C.S., Levasseur, M., Marchetti, A., Millero, F.J., Nishioka, J., Nojiri, Y., van Oijen, T., Riebesell, U., Rijkenberg, M.J.A., Saito, H., Takeda, S., Timmermans, K.R., Veldhuis, M.J.W., Waite, A.M., Wong, C.S., 2005. Synthesis of iron fertilization experiments: from the iron age in the age of enlightenment. J. Geophys. Res.—Oceans 110, C09S16.

DiTullio, G.R., Garcia, N., Riseman, S.F., Sedwick, P.N., 2007. Effects of iron concentration on pigment composition in *Phaeocystis antarctica* grown at low irradiance. Biogeochemistry 83, 71–81.

DiTullio, G.R., Grebmeier, J.M., Arrigo, K.R., Lizotte, M.P., Robinson, D.H., Leventer, A., Barry, J.B., VanWoert, M.L., Dunbar, R.B., 2000. Rapid and early export of *Phaeocystis antarctica* blooms in the Ross Sea, Antarctica. Nature 404, 595–598.

Ducklow, H.W., Baker, K., Martinson, D.G., Quetin, L.B., Ross, R.M., Smith, R.M., Stammerjohn, S.E., Vernet, M., Fraser, W., 2007. Marine pelagic systems: the West Antarctic Peninsula. Philosophical Transactions of the Royal Society B Biological Sciences 362, 67–94.

Fitzwater, S.E., Johnson, K.S., Gordon, R.M., Coale, K.H., Smith, W.O., 2000. Trace metal concentrations in the Ross Sea and their relationship with nutrients and phytoplankotn growth. Deep-Sea Res. II 47, 3159–3179.

Fragoso, G.M., Smith Jr., W.O., 2012. Influence of hydrography on phytoplankton distribution in the Amundsen and Ross Seas, Antarctica. Journal of Marine Systems 89, 19–29.

Gerringa, L.J.A., Alderkamp, A.-C., Laan, P., Thuróczy, C.-E., De Baar, H.J.W., Mills, M.M., Van Dijken, G.L., Van Haren, H., Arrigo, K.R., 2012. Iron from melting glaciers fuels the phytoplankton blooms in Amundsen Sea (Southern Ocean); iron biogechemistry. Deep-Sea Res. II 71–76, 16–31.

Hellmer, H.H., Jacobs, S.S., Jenkins, A., 1998. Oceanic erosion of a floating Antarctic glacier in the Amundsen Sea. Antarct. Res. Ser. 75, 83–99.

Holm-Hansen, O., Lorenzen, C.J., Holmes, R.W., Strickland, J.D.H., 1965. Fluorometric determination of chlorophyll. J. Cons. Perm. Int. Explor. Mer. 30, 3–15.

Jacobs, S.S., Jenkins, A., Giulivi, C.F., Dutrieux, P., 2011. Stronger ocean circulation and increasing melting under Pine Island Glacier ice shelf. Nature Geosciences 4, 519–523.

Jacobs, S.S., Hellmer, H.H., Jenkins, A., 1996. Antarctic ice sheet melting in the Southeast Pacific. Geophysical Research Letters 23, 957–960.
Jenkins, A., Dutrieux, P., Jacobs, S.S., McPhail, S.D., Perrett, J.R., Webb, A.T., White, D., 2010. Observations beneath Pine Island Glacier in West Antarctica and implications for its retreat. Nature Geoscience 3, 468–472.
Jenkins, A., Vaughan, D.G., Jacobs, S.S., Hellmer, H.H., Keys, J.R., 1997. Glaciological and oceanographic evidence of high melt rates beneath Pine island glacier, west Antarctica. Journal of Glaciology 43, 114–121.
Johnson, Z., Barber, R.T., 2003. The low-light reduction in the quantum yield of photosynthesis: potential errors and biases when calculating the maximum quantum yield. Photosynthesis Research 75, 85–95.
Karl, D.M., Christian, J.E., Dore, J.E., Letelier, R.M., 1996. Microbiological oceanography in the region west of the Antarctic Peninsula: microbial dynamics, nitrogen cycle and carbon flux. In: Foundations for Ecological ResearchWest of the Antarctic Peninsula. Antarct. Res. Ser. 70, 303–332.
Kirk, J.T.O., 1994. Light and Photosynthesis in Aquatic Ecosystems. Cambridge University Press.
Kishino, M., Takahashi, M., Okami, N., Ichimura, S., 1985. Estimation of the spectral absorption-coefficients of phytoplankton in the Sea. Bull. Mar. Sci. 37, 634–642.
Klunder, M., Laan, P., Middag, R., De Baar, H.J.W., 2011. Dissolved iron in the Southern Ocean (Atlantic sector). Deep-Sea Research II-Topical Studies in Oceanography 58, 2678–2694.
Kozlowski, W.A., Deutschman, D., Garibotti, I., Trees, C., & Vernet, M. 2011. An evaluation of the application of CHEMTAX to Antarctic coastal pigment data. Deep-Sea Research I-Oceanographic Research Papers 58: 350–364.
Kraay, G.W., Zapata, M., Veldhuis, M.J.W., 1992. Separation of chlorophylls-C1, chlorophylls-C2, and chlorophylls-C3 of marine-phytoplankton by reversed-phase-C18 high-performance liquid-chromatography. J. Phycol. 28 708–712
Krause, G.H., Weis, E., 1991. Chlorophyll fluorescence and photosynthesis—the basics. Annual Review of Plant Physiology and Plant Molecular Biology 42, 313–349.
Kropuenske, L.R., Mills, M.M., Van Dijken, G.L., Bailey, S., Robinson, D.H., Welschmeyer, N.A., Arrigo, K.R., 2009. Photophysiology in two major Southern Ocean phytoplankton taxa: photoprotection in *Phaeocystis antarctica* and *Fragilariopsis cylindrus*. Limnol. Oceanogr. 54, 1176–1196.
Lannuzel, D., Schoemann, V., De Jong, J., Pasquer, B., Van der Merwe, P., Masson, F., Tison, J.L., Bowie, A., 2010. Distribution of dissolved iron in Antarctic sea ice: spatial, seasonal, and inter-annual variability. J. Geophys. Res.—Biogeosci. 115, G03022. http://dx.doi.org/:10.1029/2009JG001031.
Leventer, A., 2003. Particulate flux from sea ice in Polar waters. In: Thomas, D.N., Dieckman., G.S. (Eds.), Sea ice—An Introduction to its Physics, Chemistry, Biology and Geology. Blackwell, Oxford, pp. 303–332.
Lewis, M.R., Smith, J.C., 1983. A small volume, short-incubation-time method for measurement of photosynthesis as a function of incident irradiance. Mar. Ecol. Prog. Ser. 13, 99–102.
Long, M.C., Dunbar, R.B., Tortell, P.D., Smith, W.O., Mucciarone, D.A., Ditullio, G.R., 2011. Vertical structure, seasonal drawdown, and net cummunity production in the Ross Sea, Antarctica. Journal of Geophysical research 116, C 10029. http://dx.doi.org/:10.1029/2009JC005954.
Mackey, M.D., Mackey, D.J., Higgins, H.W., Wright, S.W., 1996. CHEMTAX—a program for estimating class abundances from chemical markers: application to HPLC measurements of phytoplankton. Mar. Ecol. Prog. Ser. 144, 265–283.
Mangoni, O., Saggiomo, M., Modigh, M., Catalano, G., Zingone, A., Saggiomo, V., 2009. The role of platelet ice microalgae in seeding phytoplankton blooms in Terra Nova Bay (Ross Sea, Antarctica): a mesocosm experiment. Polar Biology 32, 311–323.
Mills, M.M., ALderkamp, A.-C., Thuróczy, C.-E., Van Dijken, G.L., De Baar, H.J.W., Arrigo, K.R., 2012. Phytoplankton biomass and pigment responses to Fe amendments in the Pine Island and Amundsen polynyas. Deep-Sea Res. II 71–76, 61–76.
Mills, M.M., Kropuenske, L.R., Van Dijken, G.L., Alderkamp, A.-C., Berg, G.M., Robinson, D.H., Welschmeyer, N.A., Arrigo, K.R., 2010. Photophysiology in two Southern Ocean phytoplankton taxa: photosynthesis of *Phaeocystis antarctica* (Prymnesiopheceae) and *Fragilariopsis cylindrus* (Bacillariophyceae) under simulated in situ mixed-layer irradiance. J. Phycol. 46, 1114–1127.
Mitchell, B.G., Brody, E.A., Holm-Hansen, O., McClain, C., Bishop, J., 1991. Light limitation of phytoplankton biomass and macronutrient utilization in the Southern Ocean. Limnology and Oceanography 36, 1662–1677.
Mitchell, B.G. & Kiefer, D.A. 1988. Chlorophyll-alpha specific absorption and fluorescence excitation-spectra for light-limited phytoplankton. Deep-Sea Research Part A-Oceanographic Research Papers 35: 639–663.
Nejstgaard, J.C., Tang, K.W., Steinke, M., Dutz, J., Koski, M., Antajan, E., Long, J.D., 2007. Zooplankton grazing on *Phaeocystis*: a quantitative review and future challenges. Biogeochemistry 83, 147–172.
Nelson, D.M., Smith, W.O., 1991. Sverdrup revisited—critical depths, maximum chlorophyll levels, and the control of Southern Ocean productivity by the irradiance-mixing regime. Limnology and Oceanography 36, 1650–1661.
Nitsche, F.O., Jacobs, S.S., Larter, R.D., Gohl, K., 2007. Bathymetry of the Amundsen Sea continental shelf: implications for geology, oceanography, and glaciology. Geochem. Geophys. Geosyst. 8, Q10009. http://dx.doi.org/:10.1029/2007GC001694.
Platt, T., Gallegos, C.L., Harrison, W.G., 1980. Photoinhibition of photosynthesis in natural assemblages of marine-phytoplankton. J. Mar. Res. 38, 687–701.
Pritchard, H.D., Arthern, R.J., Vaughan, D.G., Edwards, L.A., 2009. Extensive dynamic thinning on the margins of the Greenland and Antarctic ice sheets. Nature 461, 971–975.
Raiswell, R., 2011. Iceberg-hosted nanoparticulate Fe in the Southern Ocean: mineralogy, origin, dissolution kinetics and source of bioavailable Fe. Deep-Sea Res. II—Topical Studies in Oceanography 58, 1364–1375.
Raiswell, R., Benning, L.G., Tranter, M., Tulaczyk, S., 2008. Bioavailable iron in the Southern Ocean: the significance of the iceberg conveyor belt. Geochem. Trans. 9, 7. http://dx.doi.org/:10.1186/1467-4866-9-7.
Raiswell, R., Tranter, M., Benning, L.G., Siegert, M., De'ath, R., Huybrechts, P., Payne, T., 2006. Contributions from glacially derived sediment to the global iron (oxyhydr)oxide cycle: implications for iron delivery to the oceans. Geochim. Cosmochim. Acta 70, 2765–2780.
Riley, G.A., 1957. Phytoplankton of the North Central Sargasso Sea, 1950–52. Limnol. Oceanogr. 2, 252–270.
Schoemann, V., Becquevort, S., Stefels, J., Rousseau, V., Lancelot, C., 2005. *Phaeocystis* blooms in the global ocean and their controlling mechanisms: a review. J. Sea Res. 53, 43–66.
Sedwick, P.N., DiTullio, G.R., 1997. Regulation of algal blooms in Antarctic shelf waters by the release of iron from melting sea ice. Geophysical Research Letters 24, 2515–2518.
Sedwick, P.N., DiTullio, G.R., Mackey, D.J., 2000. Iron and manganese in the Ross Sea, Antarctica: seasonal iron limitation in Antarctic shelf waters. J. Geophys. Res.—Oceans 105, 11321–11336.
Shaw, T.J., Raiswell, R., Hexel, C.R., Vu, H.P., Moore, W.S., Dudgeon, R., Smith Jr, K.L., 2011. Input, composition, and potential impact of terrigenous material from free-drifting icebergs in the Weddell Sea. Deep-Sea Research 58, 1376–1383.
Shields, A.R., Smith, W.O., 2009. Size-fractionated photosynthesis/irradiance relationships during *Phaeocystis antarctica*-dominated blooms in the Ross Sea, Antarctica. Journal of Plankton Research 31, 701–712.
Smith, W.O., Asper, V.A., 2000. A balanced nitrogen budget of the surface layer of the southern Ross Sea, Antarctica. Geophys. Res. Lett. 27, 2721–2724.
Smith, W.O., Shields, A.R., Peloquin, J.A., Catalano, G., Tozzi, S., Dinniman, M.S., Asper, V.A., 2006. Interannual variations in nutrients, net community production, and biogeochemical cycles in the Ross Sea. Deep-Sea Res. II—Topical Studies in Oceanography 53, 815–833.
Smith, W.O., Dinniman, M.S., Tozzi, S., DiTullio, G.R., Mangoni, O., Modigh, M., Saggiomore, V., 2010. Phytoplankton photosynthetic pigmetns in the Ross Sea: pattern and relationships among functional groups. J. Mar. Syst. 82, 177–185.
Smith, W.O., Nelson, D.M., 1986. The importance of ice-edge phytoplankton blooms in the Southern Ocean. Bioscience 36, 251–257.
Smith, W.O., Shields, A.R., Dreyer, J.C., Peloquin, J.A., Asper, V., 2011. Interannual variability in vertical export in the Ross Sea: magnitude, composition, and environmental correlates. Deep-Sea Res. I 58, 147–159.
Strutton, P.G., Griffiths, F.B., Waters, R.L., Wright, S.W., Bindoff, N.L., 2000. Primary productivity off the coast of East Antarctica (80–150° E): January to March 1996. Deep-Sea Res. II—Topical Studies in Oceanography 47, 2327–2362.
Sverdrup, H.U., 1953. On conditions for the vernal blooming of phytoplankton. J. Cons. Int. Explor. Mer. 18, 287–295.
Sweeney, C., Smith, W.O., Hales, B., Bidigare, R.R., Carlson, C.A., Codispoti, L.A., Gordon, L.I., Hansell, D.A., Millero, F.J., Park, M.O., Takahashi, T., 2000. Nutrient and carbon removal ratios and fluxes in the Ross Sea, Antarctica. Deep-Sea Res. II—Topical Studies in Oceanography 47, 3395–3421.
Tagliabue, A., Arrigo, K.R., 2003. Anomalously low zooplankton abundance in the Ross Sea: an alternative explanation. Limnol. Oceanogr. 48, 686–699.
Tagliabue, A., Arrigo, K.R., 2005. Iron in the Ross Sea: 1. Impact on CO_2 fluxes via variation in phytoplankton functional group and non-Redfield stoichiometry. J. Geophys. Res.—Oceans 110, C03009. http://dx.doi.org/:10.1029/2004JC002531.
Thuróczy, C.-E., Alderkamp, A.-C., Laan, P., Gerringa, L.J.A., De Baar, H.J.W., Arrigo, K.R., 2012. Key role of organic complexation of iron in sustaining the phytoplankton blooms in th ePine Island and Amundsen Polynyas (Southern Ocean). Deep-Sea Res. II 71–76, 49–60.
Tison, J.L., Brabant, F., Dumont, I, Stefels, J., 2010. High resolution dimethylsulfide and dimethylsulfoniopropionate time series profiles in decaying summer first-year sea ice at Ice Station Polarstern, western Weddell Sea, Antarctica. J. Geophys. Res.—Earth Surf. 115, G04044.
Tortell, P.D., Long, M.C., Payne, C.P., Alderkamp, A.,-C., Arrigo, K.R., 2012. Spatial distribution of p CO_2, ΔO_2/Ar and dimethylsulfide (DMS) in Polynya waters and the sea ice zone of the Amundsen Sea, Antarctica. Deep-Sea Res. II 71–76, 77–93.
Van Hilst, C.M., Smith, W.O., 2002. Photosynthesis/irradiance relationships in the Ross Sea, Antarctica, and their control by phytoplankotn assemblage composition and environmental factors. Mar. Ecol. Prog. Ser. 226, 1–12.
Van Leeuwe, M.A., Stefels, J., 2007. Photosynthetic responses in *Phaeocystis antarctica* towards varying light and iron conditions. Biogeochemistry 83, 61–70.
Van Leeuwe, M.A., Villerius, L.A., Roggeveld, J., Visser, R.J.W., Stefels, J., 2006. An optimized method for automated analysis of algal pigments by HPLC. Mar. Chem. 102, 267–275.
Vernet, M., Martinson, D., Iannuzzi, R., Stammerjohn, S., Kozlowski, W., Sines, K., Smith, R., Garibotti, I., 2008. Primary production within the sea-ice zone west of the Antarctic Peninsula: I-sea ice, summer mixed layer, and irradiance. Deep-Sea Res. II 55, 2068–2085.
Walker, D.P., Brandon, M.A., Jenkins, A., Allen, J.T., Dowdeswell, J.A., Evans, J., 2007. Oceanic heat transport onto the Amundsen Sea shelf through a submarine

glacial trough. Geophys. Res. Lett. 34, L02602. http://dx.doi.org/:10.1029/2006GL028154.

Webb, W.L., Newton, M., Starr, D., 1974. Carbon-dioxide exchange of Alnus-Rubra—mathematical-model. Oecologia 17, 281–291.

Wright, S.W., Thomas, D.P., Marchant, H.J., Higgins, H.W., Mackey, M.D., Mackey, D.J., 1996. Analysis of phytoplankton of the Australian sector of the Southern Ocean: comparisons of microscopy and size frequency data with interpretations of pigment HPLC data using the 'CHEMTAX' matrix factorisation program. Mar. Ecol.—Prog. Ser. 144, 285–298.

Wright, S.W., Van den Enden, R.L., Pearce, I., Davidson, A.T., Scott, F.J., Westwood, K.J., 2010. Phytoplankton community structure and stocks in the Southern Ocean (30–80° E) determined by CHEMTAX analysis of HPLC pigment signatures. Deep-Sea Res. II—Topical Studies in Oceanography 57, 758–778.

Zapata, M., Jeffrey, S.W., Wright, S.W., Rodriguez, F., Garrido, J.L., Clementson, L., 2004. Photosynthetic pigments in 37 species (65 strains) of Haptophyta: implications for oceanography and chemotaxonomy. Mar. Ecol.—Prog. Ser. 270, 83–102.